A State-of-the-Art Review on Direct Welding of Polymer to Metal for Structural Applications: Part 1 — Promising Processes

BY A. S. KHAN, P. DONG, F. LIU, AND Y. ZHANG

Abstract

Structural lightweighting through the effective use of multiple materials has received increasing attention for fulfilling today's demands for environmental sustainability in transportation systems. Direct dissimilar material joining methods (versus, e.g., traditional adhesive bonding or mechanical fastening) have become increasingly desirable since they offer process simplicity, production efficiency, and hermetic sealing, among others. In this two-part article, we provide a critical assessment of the state-of-the-art research and promising direct dissimilar material joining techniques reported over the last decades, with a particular emphasis on their potential for structural applications in Part I. As such, recent advances in advanced joint design and modeling methods for enabling optimum joint design for jointability and joint performance are presented along with some detailed examples for demonstrating their potential impacts on industrial applications in Part II. Finally, recommendations on future research and development directions are outlined for supporting the industry's drive towards multi-material lightweighting.

Keywords

- Dissimilar Materials Joining
- Polymer to Metal Direct Welding
- Welding
- Joint Property
- Chemical Bonding

Introduction

To ensure sustainability of the environment and quality of life, effective use and reuse of existing materials have become increasingly important in transitioning to a circular economy (Refs. 1–3). As part of such an effort, major automotive manufacturers have been leading the drive toward structural lightweighting over the last decade or so (Refs. 4–7). The consensus resulting from recent major research initiatives is that multi-material structure, i.e., "using the right material at the right place," offers the most effective lightweighting in addition to achieving multi-functionalities (Refs. 8–12]). For instance, the US Department of Energy (DOE) multi-material lightweight vehicle (MMLV) autobody structure (Ref. 13), made of high-strength steel, aluminum, magnesium alloys, and carbon fiber polymer composites can offer up to 40% weight reduction versus all high-strength steel structures, as highlighted in Fig 1. However, the challenge has been how to cost-effectively manufacture such multi-material structures in a mass-production environment while ensuring structural durability, and recyclability. Traditional mechanical fastening incurs additional part counts and adds weight while adhesive bonding increases production cycle time in addition to its implications for long-term durability and recyclability of adhesive-bonded components (Refs. 14–16). To mitigate some of the major concerns, direct welding of dissimilar materials (polymer to metal or between incompatible metals, e.g., aluminum to steel) has gained growing attention in the research community over recent years (Refs. 17–19).

There have been some promising successes in developing methods for direct welding of polymer or polymer-composite to metal. For instance, Liu et al. (Ref. 20) demonstrated that the functional groups in polyamide (PA) or nylon enabled its direct welding with aluminum alloy without any surface or material pre-treatment through a carbon-oxygen-metal (aka C-O-M) chemical bond formation under localized heating and pressure conditions, e.g., via a friction-assisted lap welding technique. Using the friction-assisted spot method, Khan et al. (Ref. 21) recently demonstrated that a nonpolar polypropylene (PP) composite can be directly welded using a thin layer of functional group seeding material between the PP composite and metal partner without special surface treatments. Han et al. (Ref. 22) have shown the joining of PP sheet with aluminum alloy using a metal surface laser texturing by micromechanical interlocking under friction-assisted spot joining. Kawahito et al. (Ref. 23) have shown successful joining of steel and PA under pulsed laser joining and achieved strong joints. The combination of PA or PP and aluminum or steel can be used to reduce weight in some of the automotive interior components. As shown in Fig. 2A, recent applications of PP
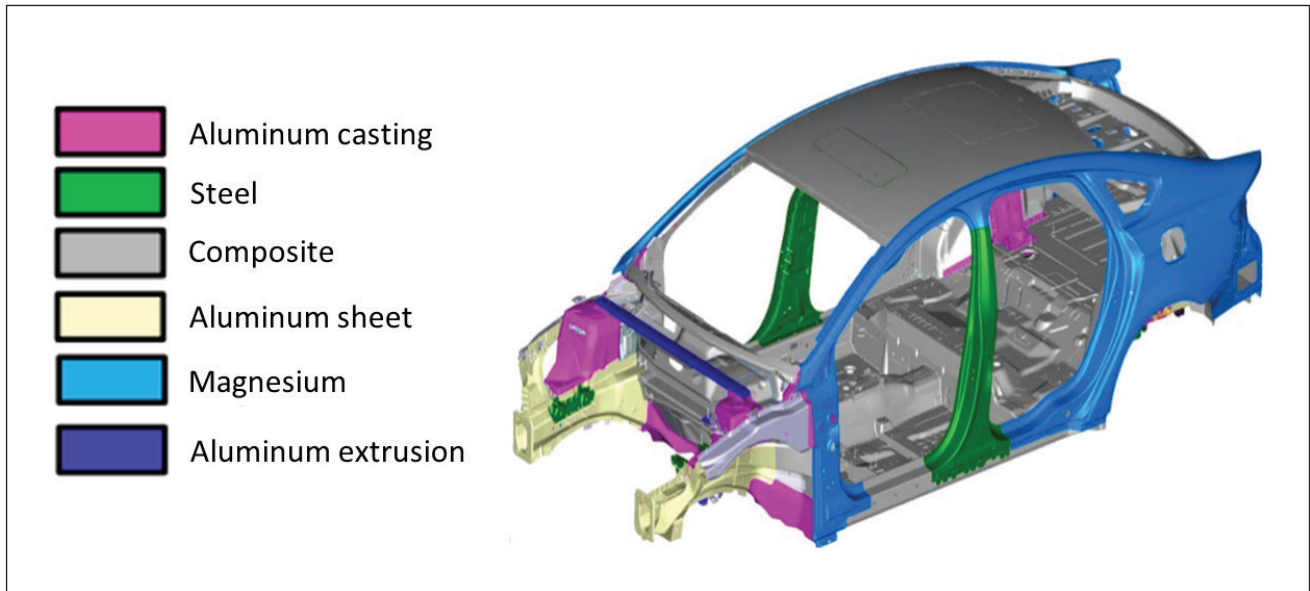
Fig. 1 — Structural lightweighting through a multi-material concept (Ref. 13).
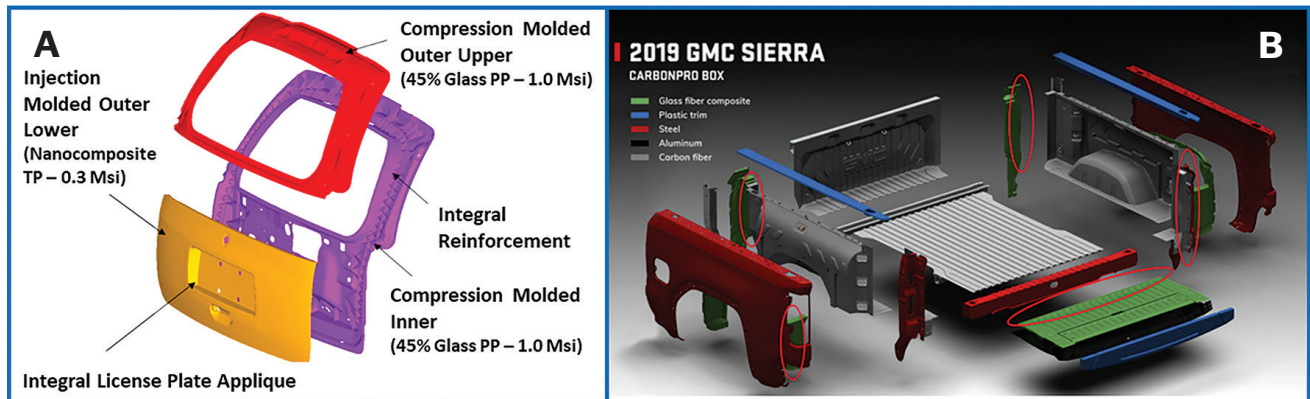
Fig. 2 — A — A lightweight liftgate concept made of GFPP of passenger van (Ref. 43); B — a lightweight truck cargo bed made of a metal-polymer hybrid structure (gmauthority.com).

in GM liftgates and PA composites in GMC Sierra trucks (Fig. 2B) have shown the importance of directly joining polymer composites with aluminum and steel structures for structural lightweight applications in mass production environments.

It should be noted that the direct joining of incompatible dissimilar metals such as aluminum alloys to steel (involved in MMLV in Fig. 1) has been facing similar challenges due to the formation of brittle intermetallic compounds (IMCs) at the joining interface (Refs. 24–26). Recent research efforts have shown that brittle IMCs can be effectively avoided through a nanoscale shear localization process beyond a threshold strain rate under certain friction stir welding conditions. As a result, the aluminum-steel interface exhibits a dominantly amorphous microstructure which offers high interfacial bonding strength and excellent thermal stability (Refs. 27–30). Good thermal stability is important to restrict the nucleation and growth of IMCs at thermal cyclic loading conditions (Ref. 148).

The use of fiber-reinforced thermoplastics has been a prime mover in the automotive industries due to recyclability (Refs. 31–34) and has been seeing an uptake in aerospace and marine structures as well (Refs. 35–38). It is expected that the need for recyclable polymers and lightweighting requirements will enable the use of thermoplastics for as much as up to 40% of the total material in automotive structures (Refs. 13, 39). PA and PP are the most common polymer materials being used in the automotive industries due to their formability, low cost, and recyclability (Refs. 40–43). PP, due to its low density compared with other industrial polymers and high corrosion resistance, is widely used in the automotive industry (Refs. 44–47). The direct joining of metals with polymer or polymer composites thus eliminates multiple process steps, mechanical fasteners, and adhesives and provides strong joints capable of hermetic sealing required for applications under pressure and severe weather environments (Refs. 17–19). As recently suggested by some recent studies (Refs. 48–50), direct dissimilar material joining
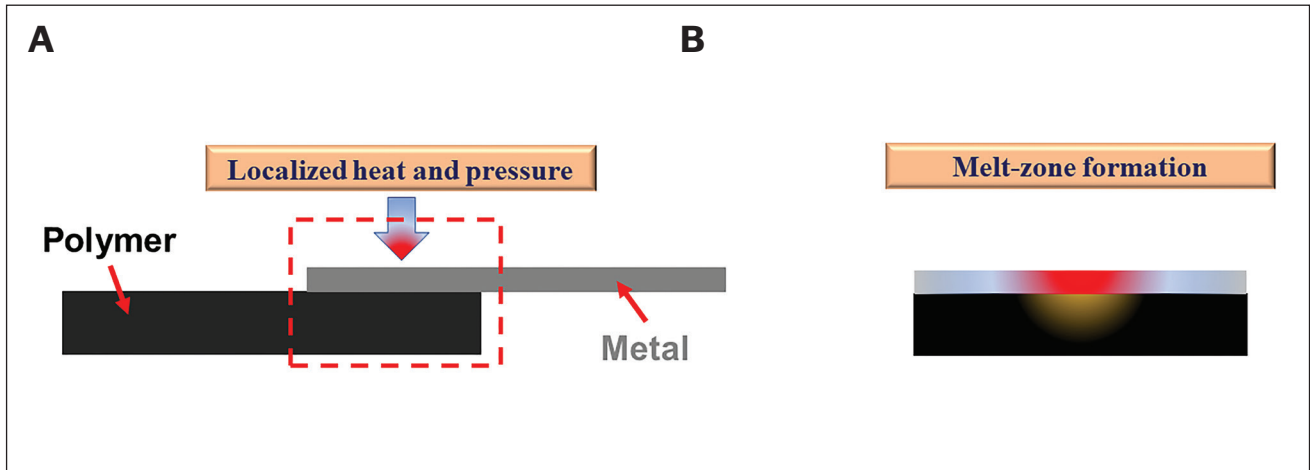
Fig. 3 — Schematic of localized heat and pressure conditions to join metal and polymer.
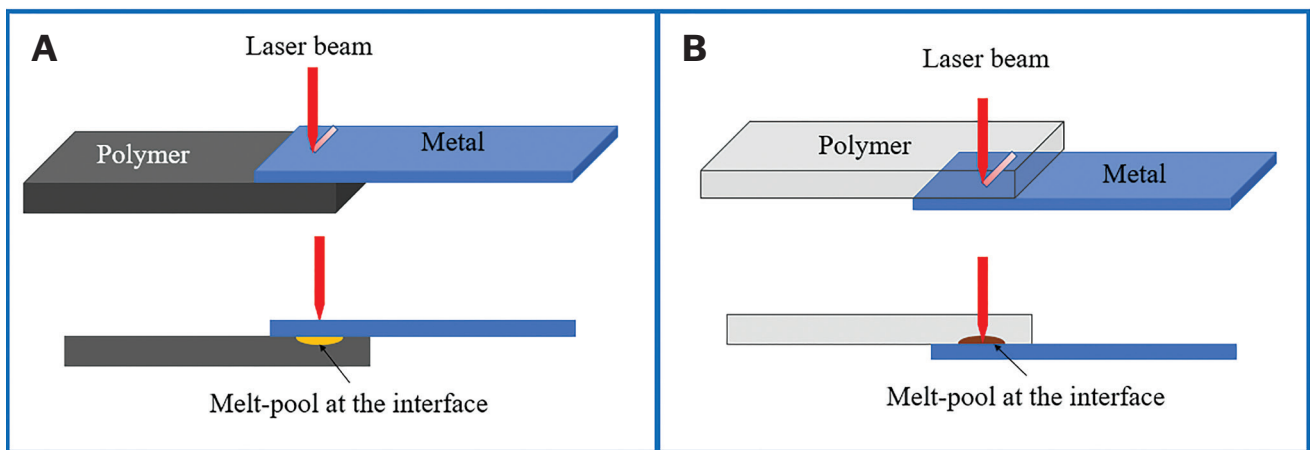
Fig. 4 — Variants of laser-assisted joining: A — Conduction joining; B — transmission joining.

also offers improved structural reliability under dynamic and fatigue loading conditions.

As highlighted above, multi-material or mixed-material structures made of dissimilar metals, polymers, and polymeric composites have been becoming increasingly important for meeting today's increasingly stringent weight reduction, energy efficiencies, and recyclability requirements (Refs. 51, 52). However, robust, reliable, and cost-effective joining methods are still in the early research and development stage. Among various new dissimilar material joining methods under exploration today, direct joining of polymer to metal is of the most interest in the mass-production environment and can be a key enabler for realizing the advanced multi-material structures (e.g., the one shown in Fig. 1) cost-effectively. Along this line, this paper is structured as follows: After a brief introduction of the need for direct joining methods for effectively integrating polymer composites into metal for structural applications, some of the promising direct joining methods will be critically reviewed and assessed in Section 2. Their process characteristics, bonding mechanisms involved, as well chemical bonding enhancement techniques are discussed in Section 3. Then, in Section 4, some promising bonding and joint strength enhancement techniques are discussed. We

then conclude Part I of this state of the art review by identifying remaining critical research areas for achieving reliable direct polymer to metal joining enabling structural applications. As a sequel to Part I, in Part II (Ref. 149), joint property characterization methods, particularly those that are relevant for supporting computer-aided engineering (CAE) for design and structural performance evaluation will be discussed. One of the key outcomes of Part II is mechanics-based principles for achieving optimal design of dissimilar material joints for improved jointability and joint performance in load-bearing structures. Finally, some of the unresolved research issues for enabling reliable structural applications will be summarized for consideration by the research community.

Promising Direct Joining Techniques

Here, a direct joining technique is defined as a method by which a polymer or its composite forms (e.g., reinforced through glass or carbon fibers) can be joined with a metal substrate by forming chemical bonds without needing any separate surface or material pretreatment or curing process (Ref. 48). Among all promising direct joining processes
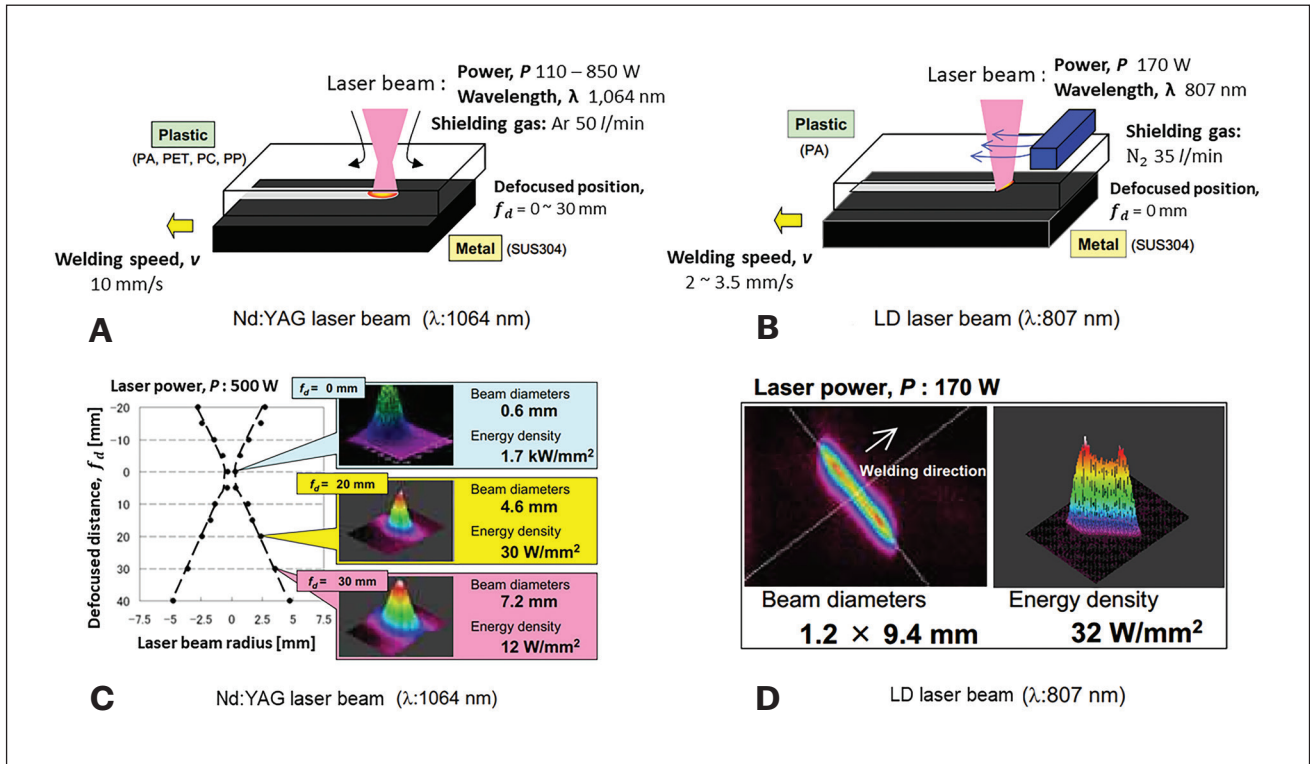
Fig. 5 — Nd:YAG vs. diode laser (LD) joining method characteristics (Ref. 23).
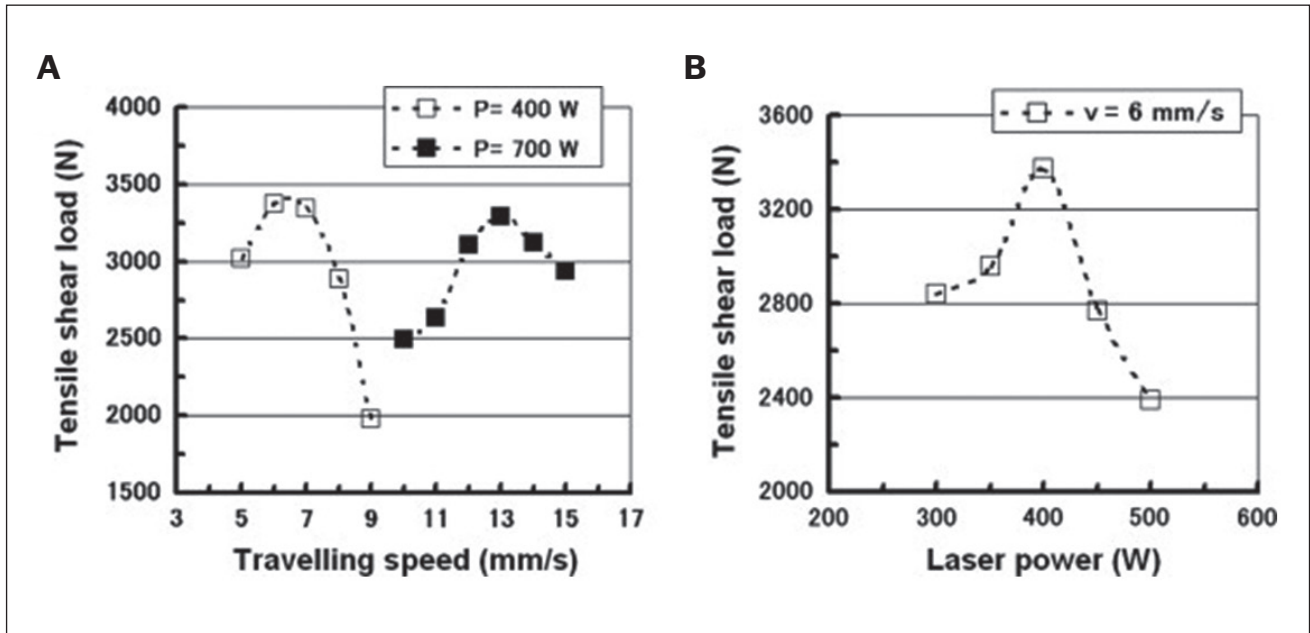
Fig. 6 — Effect of laser process parameters on joint load capacity (Ref. 60).

reported in the literature to date, localized heat and pressure are the necessary ingredients (Fig. 3) for providing favorable thermomechanical conditions for the formation of chemical bonds. In this regard, thermoplastic polymers and their composites including glass fibers and carbon fiber composites are often considered for joining with metals and their alloys. Among them, polymers with carbonyl functional groups, such as polyamide (PA) or nylon, polycarbonate (PC), and polyether ether ketone (PEEK) have been shown to possess weldability with aluminum 5xxx, 6xxx, and 7xxx alloys for automotive and aerospace applications, i.e., without needing any special surface or material treatment before joining. Whereas polymers lacking carbonyl functional groups, such as PP, and PE, typically require special surface treatment such as
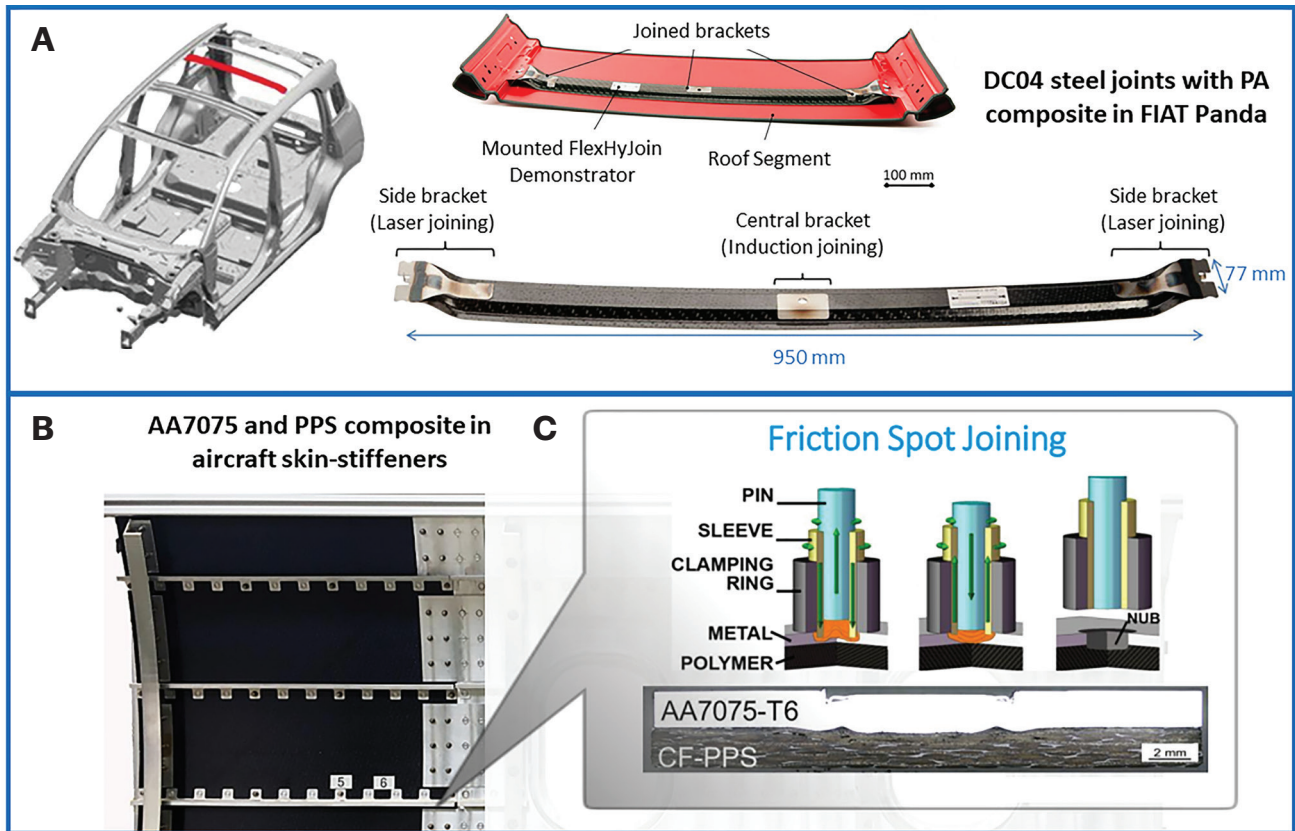
Fig. 7 — A — Fiat panda roof grill made of steel-PA composite using laser and induction joining (compositesworld. com); B and C — aircraft fuselage structure made of Al-PPS composite using friction spot joining (Refs. 17, 68).

metal surface laser texturing for mechanical interlocking or chemical treatment to enable chemical bonding with metal counterparts, therefore, continuing to pose significant challenges for achieving direct joining with metals.

For dissimilar material combinations discussed above, localized heating and pressure can be achieved through a variety of means, e.g., laser, electrical resistance, induction, ultrasonic vibration, and friction. Some of the promising direct joining processes are described and discussed below, based on their process capability, particularly for structural applications.

Laser-Assisted Joining Processes

Process Description

It utilizes a laser source to generate laser beams of suitable wavelength to project onto the metallic sheet and locally heat the interacted area. A customized clamping system is often used to provide localized pressure conditions for the molten polymer to interact with the metal sheet and form the joint. The laser beam can be projected directly on the metal surface to heat and melt the polymer (plastic) underneath (conduction joining CJ, Fig. 4A) or it can pass through a transparent polymer to heat the metal at the assembly interface (transmission joining TJ, Fig. 4B) (Refs. 23, 53).

Conduction joining (CJ) can be implemented for opaque polymers when the laser wavelength can't penetrate the polymer sheet without significantly damaging it. Laser beams can be applied either in spot configuration or linear configuration per the joint design requirements and shielding gases such as Argon (Ar) or Nitrogen (N2) are often used to protect material surfaces and control the temperature.

Key Process Parameters and Joint Formation Mechanisms

Laser beam shape, power density, laser wavelength, and scanning speed collectively affect the joining quality between a given metal and polymer combination. Laser power density is a function of laser power and defocused distance. Combined with laser beam shape and wavelength, the interaction volume or fusion zone can be controlled to provide sufficient wetting of the metal surface with polymer. The directed laser heats the metal, and the localized rapid heating further melts and often generates inherent bubbles at the metal/polymer interface. One key consideration in such laser-assisted polymer-metal joining is the amount of bubbles formed during localized rapid heating. Such bubbles, although can help by generating pressure between the molten layer of polymer and metal substrate, in excess, lead to a poor bonding quality. For example, Kawahito et al. (Ref. 23) used a continuous wave (CW) 1.5 kW Nd:YAG laser beam with a 1064 nm wavelength and a 200W laser diode (LD) laser beam with an 807
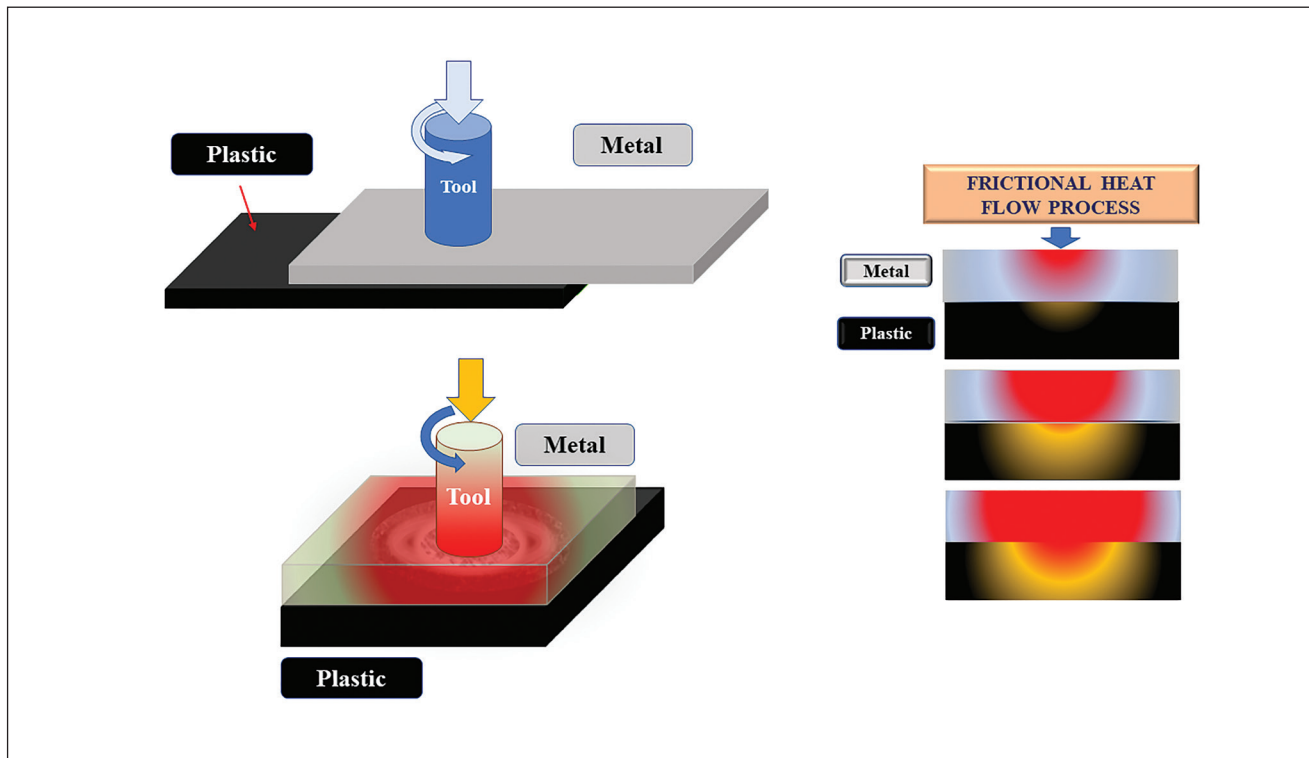
Fig. 8 — Schematic of friction-based spot joining method.

nm wavelength to join stainless steel with PA, polyethylene terephthalate (PET) and polycarbonate (PC) and used Ar and N2 as shielding gases for continuous wave and laser diode mode respectively. Gas bubble formation was found to be minimal under CJ mode for linear configuration using a laser diode laser beam while joining SUS304 and PA (Fig. 5).

Furthermore, a defocused laser beam can be used to regulate heating zone size, geometry, and beam/material interaction volume (Refs. 54–56). Consequently, a larger defocus distance increases the weld width and spreads the temperature and energy uniformly. However, an optimal defocus distance, laser power density, and spot size are often necessary, and the optimum values change for the material combination provided (Refs. 57–59). Jung et al. (Ref. 60) found that there is always an optimal laser power and scanning speed to obtain the strongest joint made of steel and nylon (PA6) composite (Fig. 6). The clamping pressure plays an indirect role during the weld formation process and can be generated by a mechanical, pneumatic or servo-electronically driven device. It is found that a minimum contact pressure to keep the joining counterparts closely in contact is necessary to achieve good interfacial bonding, resulting in stronger joints demonstrated through mechanical testing (Refs. 61–63). Applying too-high pressure can deteriorate interfacial bond quality. Metal and polymer usually have an extremely high thermal conductance difference and the application of pressure also ensures a continuous heat diffusion between these highly different materials. It also affects bubble formation and thus controls the final bond to a significant extent (Ref. 64, 65).

Joint Strength and Structural Applications

The joint strength is governed primarily by the material interaction volume and interface quality at the metal/polymer joining interface which in turn is controlled by localized heating (Refs. 66, 67). Figure 7A shows a recent application of laser joining of steel with PA composite for a FIAT panda roof grill and represents the adaptability of the laser joining method in automotive structures. To develop a continuous production throughput, the laser joining method further requires due automation and qualification for load-bearing applications.

Friction-Based Joining Processes

Process Description

Friction-based direct joining between metal and polymer shares a great deal of similarities with friction stir welding (FSW) but differs in fundamentals. The major difference is not only in the tooling pin functionality but also in geometry (Refs. 17, 69–72). It generates friction heating by rotating the friction tool against the metal part of the joint. The resulting local heating rapidly diffuses to the metal/polymer interface to cause the melting of the polymer in contact with the metal underneath the rotating friction tool. By design, such friction-based direct joining processes using rotational friction tool simultaneously produces both localized heating and pressure through the rubbing action between the rotating tool head and the metal surface. A sufficient closing contact
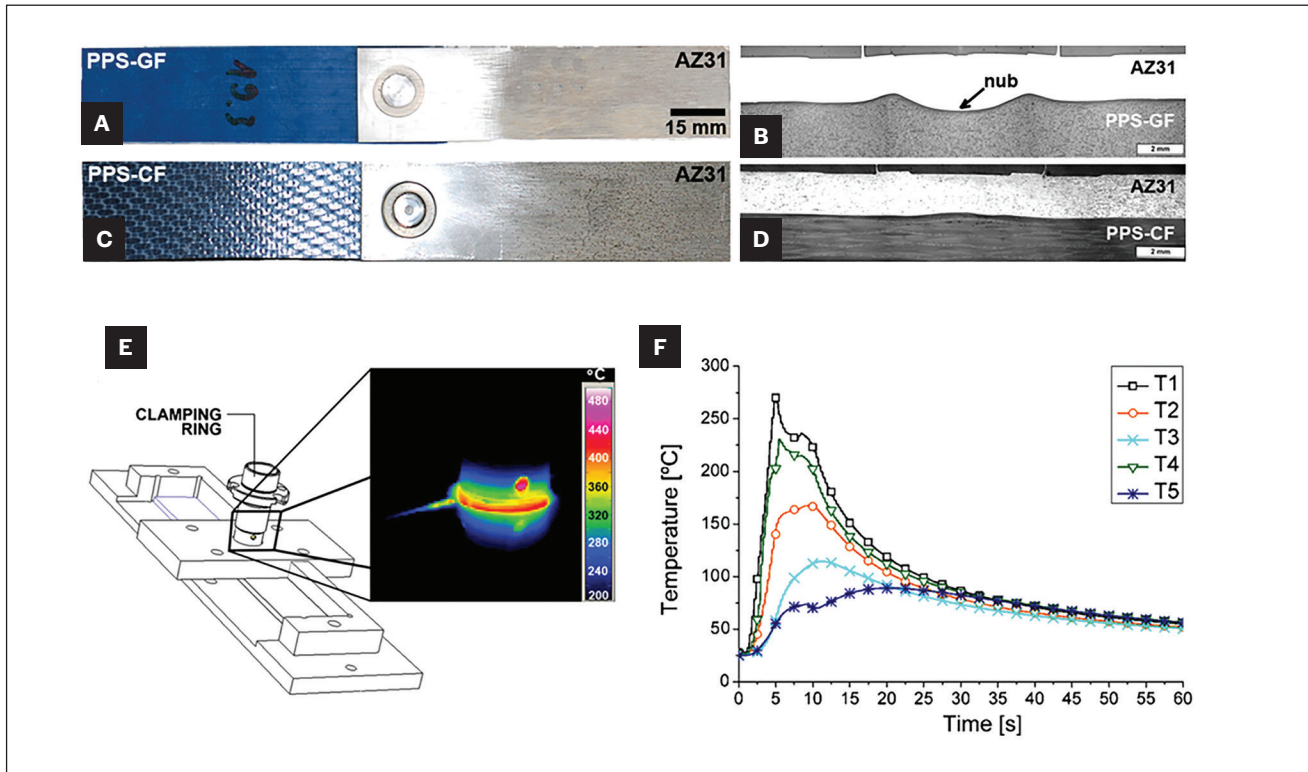
Fig. 9 — Spot joints made using the FSpJ method, cross-section, and process temperature characteristics (Ref. 71).

pressure at the joint interface is necessary to keep the joining counterparts in close contact as in the case of the laser joining. Such contact pressure can be achieved through the same unitary system (embedded with the tooling system) or by a binary system (externally via clamps or temporary fixtures). It can be used either for spot (Figs. 8 and 9) or linear (Fig. 10) joining configurations under the same principle. The linear joining configuration has been termed friction lap welding (FLW) or friction lap processing (FLP) and was initially used by Okada et al. (Ref. 147) to join metal and polymer sheets. The spot joining configuration has been termed friction spot joining (FSpJ) and has been found considerably advantageous due to its ease of process control.

Key Process Parameters and Joint Formation Mechanisms

The tool impression area, tool rotation rate, plunge force or depth, and weld time (spot time in spot joining configuration or linear welding speed in linear joining configuration) play important roles in achieving the desired joining between a given metal and polymer combination. The diffusing heat resulting from friction heating rapidly raises the polymer temperature, and the continuous heat generation raises the volumetric temperature above the bulk melting point of the polymer (Figs. 8 and 9). Thus, this molten polymer reacts with the metal surface present at the vicinity forming the chemical bond at the joint interface under the localized heat and pressure conditions. Excess temperature thermally decomposes the polymer material and deteriorates

the joining interface by introducing gaseous bubbles both in friction spot joining (FSpJ) and friction lap welding (FLW) unequivocally (Refs. 73–75). For example, Khan et al. (Ref. 21) used spot joining configuration to achieve good interfacial direct bonding between AA6061 and PP composite and found that an initial minimum contact pressure was achievable through fine-tuning the friction tool forge depth, for which 1800 RPM and 12-s spot time seemed to provide high-quality interfacial bonding, as shown in Fig. 17B. The spot weld time was found to be affecting the joint formation at a constant tool rotation rate and forge depth. Liu et al. (Ref. 72) utilized the FLW (Fig. 10) to join AA6061 and MC Nylon-6 (PA6) and achieved superior quality joints at 3000 rpm and 200 mm (7.874 in.)/min linear welding speed. The welding speed for linear welding was seen to be affecting the polymer melt pool and interfacial bond formation differently. A higher linear welding speed, although, reduced thermal energy (Fig. 11) and bubble volumes, also reduced the polymer melt pool volume. A further examination of the linear welding speed effects on joint strengths suggested that the joint strength decreased with increasing welding speed, however, not more than 22% for a 5 m (16.404 ft)/min welding speed compared to a 1 m (3.280 ft)/min welding speed (Ref. 76).

Joint Strengths and Structural Applications

Due to the lack of joint design guidelines and well-accepted strength testing methods, a common practice of using the nominal area defined by friction tool impression has been used in literature for joint strength estimation (Refs. 17, 71,
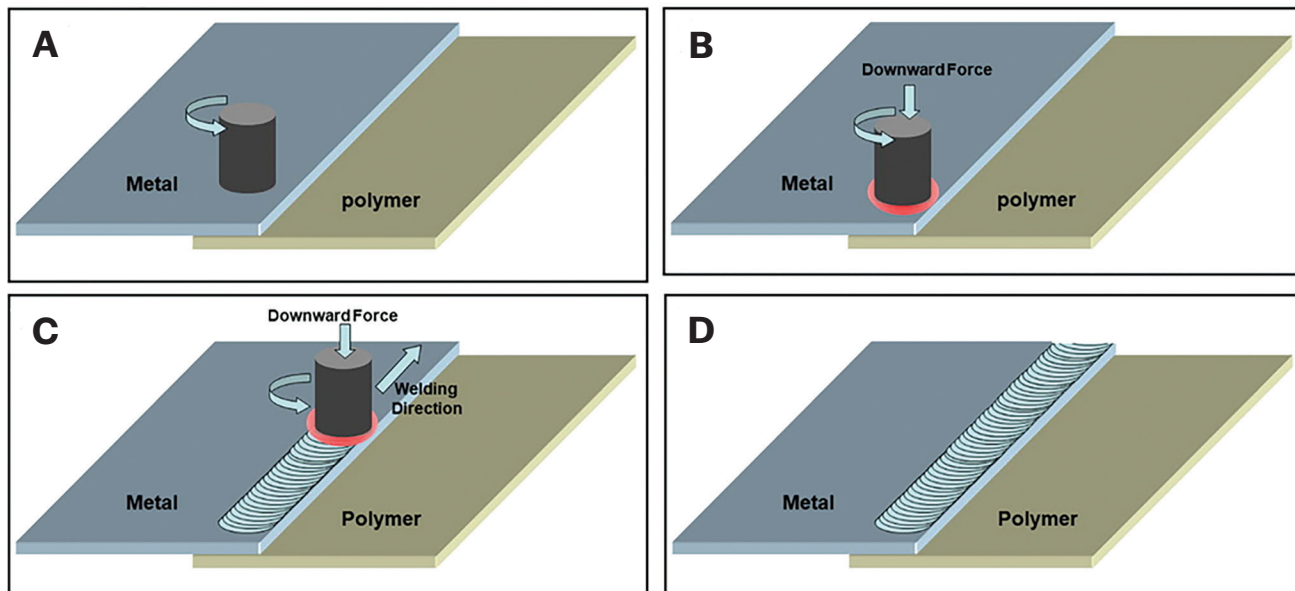
Fig. 10 — Friction lap joining schematic for metal-polymer joining (Ref. 17).

72, 77, 78). In the case of FSpJ, using the outer sleeve area the joint strength was found to be over 20 MPa for AZ31/PPS-CF joint under optimal parameters of 1950 rpm, 0.25 mm (0.010 in.) plunge depth, and 8-s spot time (Ref. 71). Under the same tooling configuration, AA2024/CF-PPS joints provided similar results although at 2900 rpm and 4.8-s spot time (Ref. 77). Figure 9 demonstrates aluminum alloy joined with the PPS composite using FSpJ in an aircraft skin panel to emphasize the adaptability of friction-based joining methods in the aircraft manufacturing industry.

Roles of Chemical Bonding

To achieve maximum joint strength in a metal-to-polymer joint, one straightforward way adopted in some of the publications is to demonstrate that a polymer-to-metal joint under lap-shear condition fails away from the weld area, e.g., across the polymer substrate, which is referred to here as a base material (BM) (Refs. 21, 78). Although this may be achieved through some of the traditional joining processes, such as adhesive bonding with sufficiently large bonding area design and/or introducing mechanical interlocking, chemical bonding at the molecular level is highly desirable for hermetic sealing purposes. Along this line, Liu et al. (Ref. 20) provided direct evidence of Al-O-C type chemical bond formation at the joining interface between PA6 and aluminum alloy, resulting in a joint strength higher than PA polymer base material. Khan et al. (Ref. 21) further achieved similar results for PP/6061 joints with a PA6-type seeding layer placed at the interface between aluminum alloy and PP composite. Such types of covalent bonds can also function as a barrier for moisture penetration through the interface to provide strong hermitic sealings. Based on these promising results, a brief discussion of various types of chemical bonding at the interface is provided in the ensuing section.

Direct Chemical Bonding Between Polymer and Metal

Role of Functional Groups

Once the necessary localized heat and pressure conditions can be achieved to melt the polymer at the polymer/metal interface, the ability to form chemical bonds is dependent on the chemical structure of the polymer under consideration. Based on the electronic charge affinity, polymers can be either functional polymers (polar polymers) or polyolefins (functionally inert or non-polar polymers) (Ref. 79). Functional polymers have active functional groups made of electronegative species, such as oxygen (-O), or nitrogen (-N), attached to the main chain or branching chain of the polymer, are hydrophilic and polar in nature, such as PA-6 (Fig. 12B). On the other hand, polyolefins do not possess any active functional group or electronegative species in or around the main chain of polymer, and are hydrophobic, functionally inert, or non-polar in nature, such as PP (Fig. 12A).

Various researchers have shown successful direct joining of polymethylmethacrylate (PMMA) (Refs. 57, 80–82), polycarbonate (PC) (Refs. 83, 84), polyethylene terephthalate (PET) (Refs. 85–88), polyamide (PA) (Refs. 72, 89–91), polyether ether ketone (PEEK) (Refs. 56, 92, 93), and polyetherimide (PEI) (Refs. 94, 95) polymers with metals. These polymers have at least one active functional group made of oxygen (-O) and thus, are polar and functionally active. Liu et. al. (Ref. 20) illustrated that functional groups like carbonyl (C = O) help develop chemical bonds with metals under optimal conditions. Thus, the direct joining with metals without any surface modifications can be effectively achieved if carbonyl (or the like) functional groups are present in the main chain of the polymer such as nylon-6 (PA6), shown in Fig. 12B. A
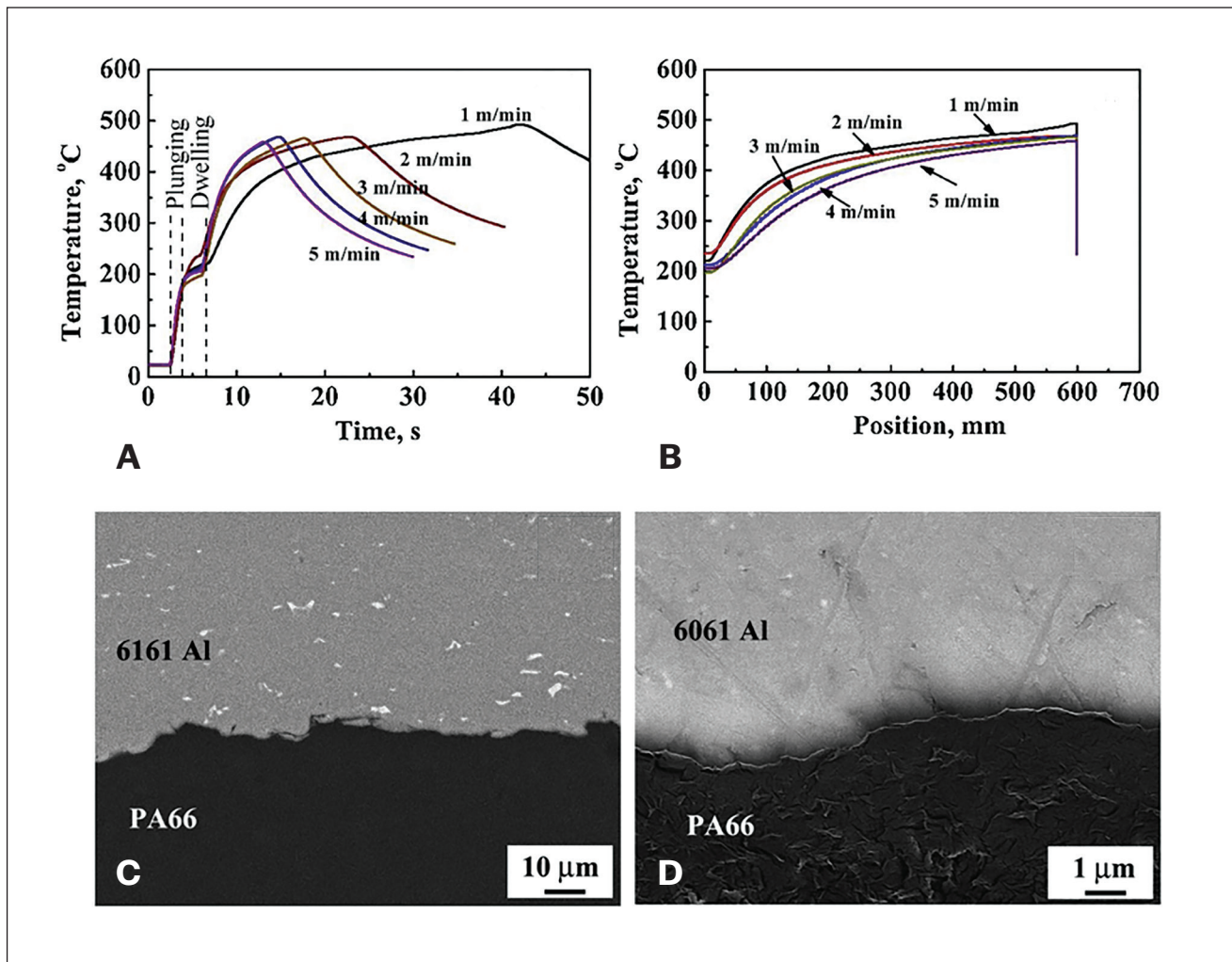
Fig. 11 — Temperature and cross-section characteristics under friction lap joining method (Ref. 78).

molecular dynamic simulation was developed which showed that 80% of the reacted C=O bonds form linear Al-O-C bonds and the rest develop a triangular Al-O-C bonding structure (Fig. 13). A further analysis using the XPS was subsequently performed, and the formation of Al-O-C chemical bond was confirmed, as shown in Figs. 12E and F.

Thermomechanical Conditions

Chemical Kinetics and C-O-M Bond Formation

Chemical bonding at the joining interface can be defined when the covalent bond formation takes place between the metal and the polymer. Physical bonding such as Van der Waals forces or hydrogen bonding can also appear at the joining interface (Refs. 18, 48, 97). Once the localized heating raises the polymer temperature to its flowable state (melting point), its polymeric chains with functional groups gain energy to actively interact with metals at the molecular level. At the same time, surface energy increases on the heated metal surface and the available carbonyl groups in the polymer develop chemical bonding to form an intimately bonded interface. Chemical bonds have a much higher bonding energy (250–1000 kJ/mol) compared to either the physical forces (2–40 kJ/mol) or hydrogen bonds (50 kJ/mol) (Ref. 98). Covalent bonds are the strongest bonds after ionic bonds among other types of bonds (Refs. 98, 99). This further substantiated the conclusion by Liu et al. (Ref. 20) that the C-O-M type covalent bonding must have taken place between metal (-M) and polymer (C=O) joining counterparts at the joining interface owing to its considerably high bonding energy (Figs. 12E and F) observed at the joint interface (Refs. 20, 78).

Another important attribute of covalent bonds is the length of the chemical bonds at the polymer-metal interface. Generally, the covalent bonds are much smaller than the water molecule ($\approx$0.27 nm across) and if the joining interface is well-developed by forming the chemical bonds at the interface, it becomes impervious to water or moisture molecules (Ref. 48). Such an interface provides strong hermetic sealing along with good load-bearing capacity to metal-polymer hybrid joints demanded for pressure containment structural applications. Additionally, the chemical bonds at the joining interface become unstable when re-heated at a sufficiently
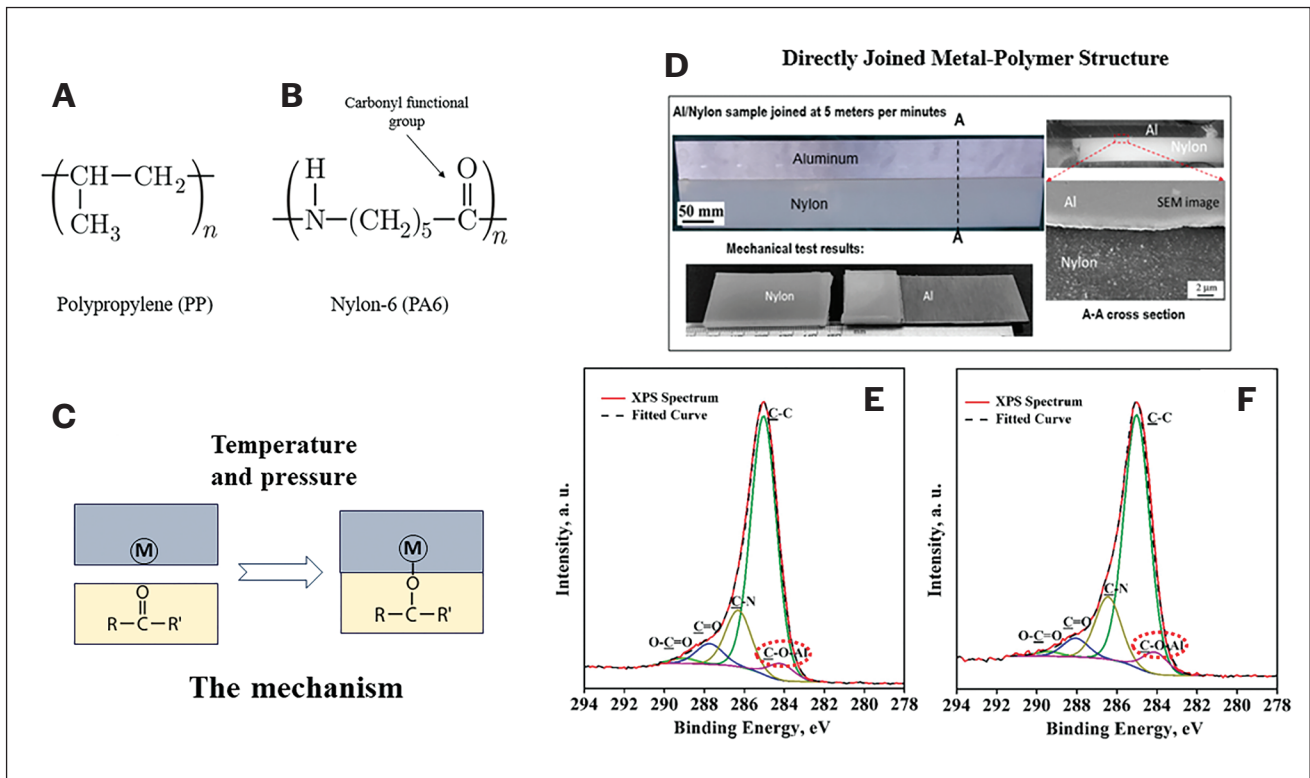
Fig. 12 — A — Non-polar polypropylene; B — PA6 with carbonyl group; C — chemical interaction at the joining interface of metal and polymer; D — AA6061 and Nylon joining under FLW and cross-section views (Ref. 20); E and F — XPS spectra confirming C-O-Al bonds at 0.8 nm and 3.2 nm depths, respectively (Ref. 78).

Captured bonding:

30% of all the C=O bond reacted with Al

80% of the reacted C=O bond forms: Al-O-C bond

20% of the reacted C=O bond forms triangular Al-O-C bond
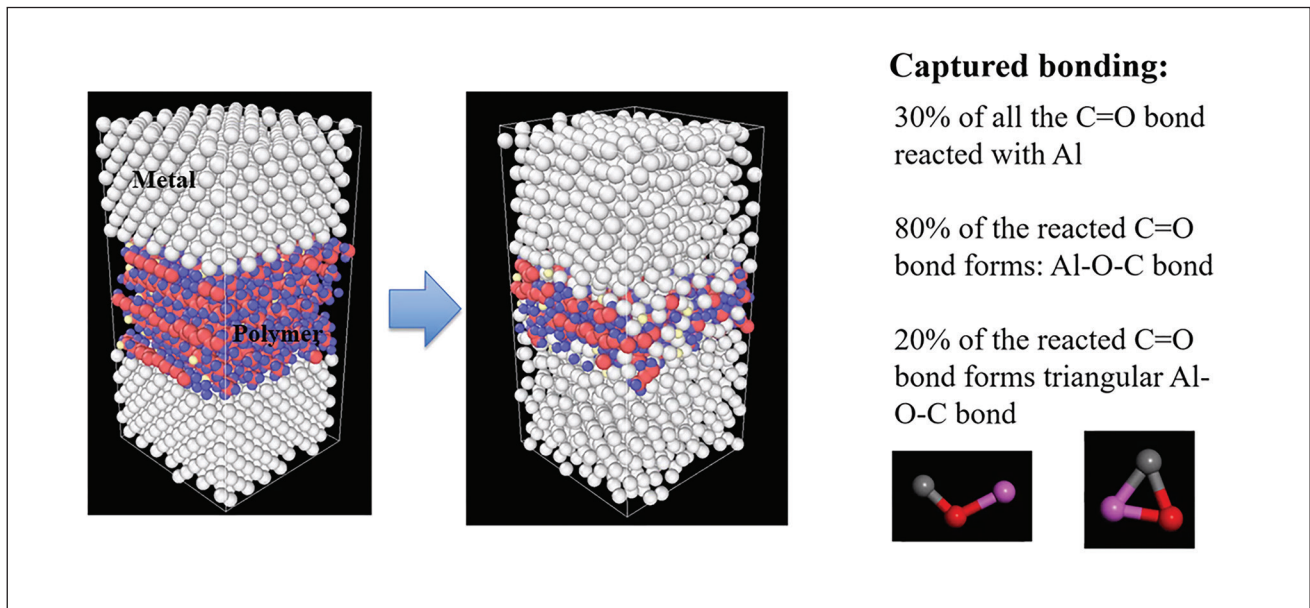
Fig. 13 — Chemical bond formation via MD simulation (Ref. 96).

high temperature above the melting point but below the degradation temperature of polymers. Such a reversible process provides an advantage to disassembly of metal-polymer hybrid joints for repair and reuse.

Alternative Chemical Bonding Possibilities

Hirchenhahn et al. (Ref. 100) have performed an interesting study and proposed another chemical bonding theory between PA66 and the native oxide of the aluminum sheet when joined using a laser joining process. They suggested that
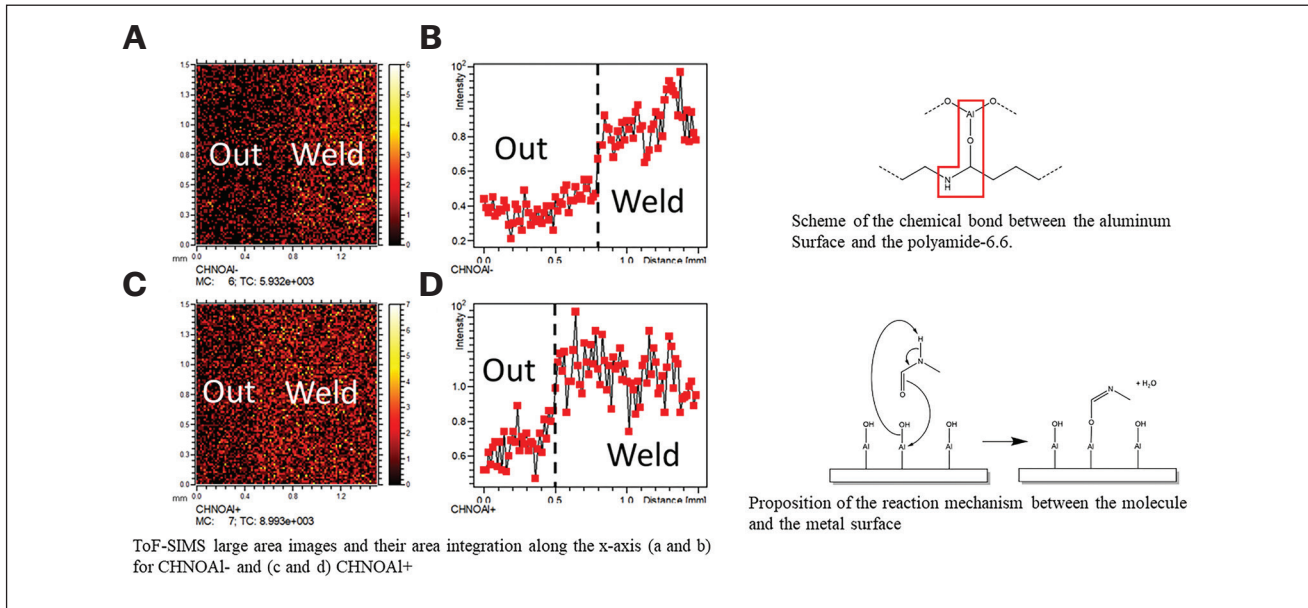
Fig. 14 — ToF-SIMS spectra near weld line for Al-PA joint and proposed model chemical reaction (Ref. 100).
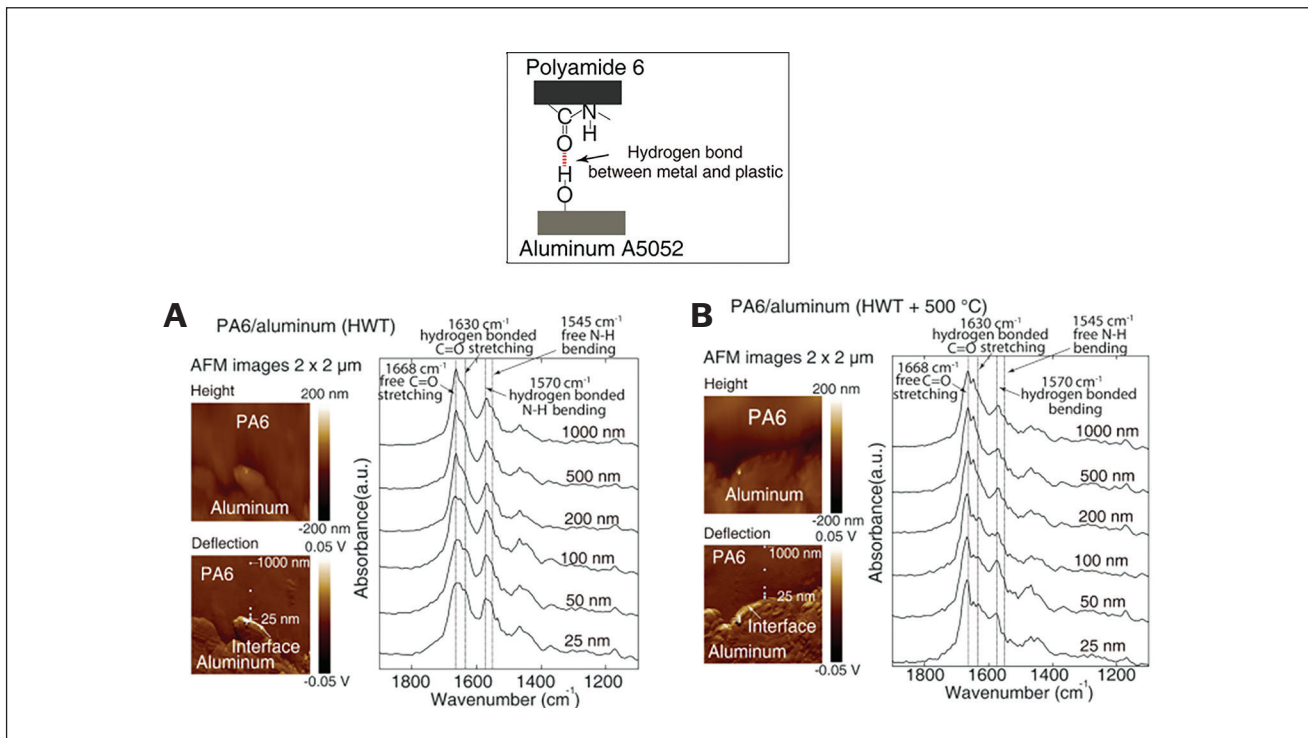
Fig. 15 — Hydrogen bond formation during Al-PA joining and IR spectra at Al-PA joint interface (Ref. 97).

the native oxide layer gets transformed into surface hydroxyl groups and then this hydroxyl group reacts with the available carbonyl group (C = O) group in the PA66 chain to formulate CHNOAl+-type species (Fig. 14). They further investigated the covalent chemical bonding between the aluminum and polymer chain using XPS and time of flight secondary electron microscopy (ToF-SIMS). In their investigation, they concluded that C-O-Al chemical bonds were indeed formed between the

carbonyl group and the available aluminum using ToF-SIMS rather than XPS. Zhao et al. (Ref. 97) have further illustrated a different bonding mechanism under injection molding of PA6 polymer over AA5052 sheets. Due to the presence of inherent oxide on the aluminum surface and susceptibility towards hydrocarbons, the formation of metal hydroxide is probable. Under such circumstances, the metal hydroxide can also contribute to chemical reaction sites. Although there
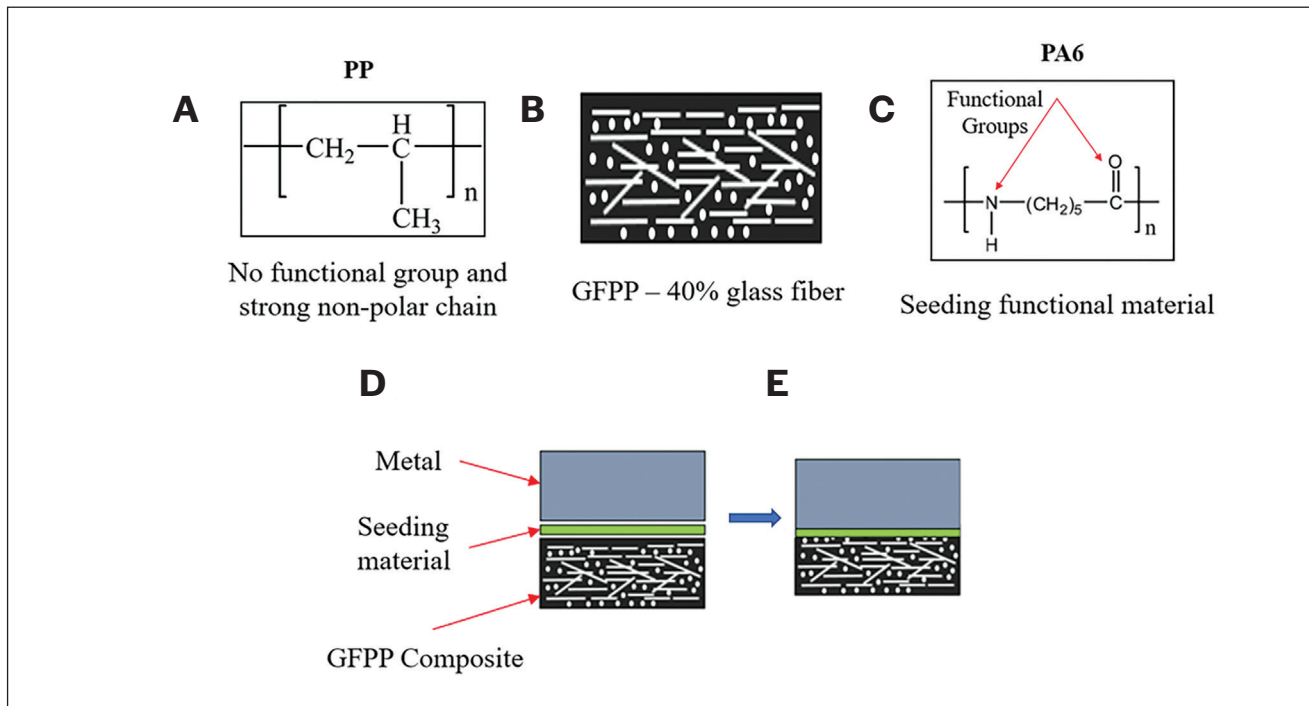
Fig. 16 — Schematic of functional group seeding methodology.

appeared a significant level of mechanical interlocking at the joint interface, they concluded that the observed joint strength was significantly enhanced by the hydrogen bonding between the -CONH (containing C=O carbonyl group) group of the PA6 and the hydroxyls (-OH) on the aluminum surface. Using AFM-IR, they confirmed the formation of hydrogen bonds at 1630 cm^{-1} wavenumber conforming with the IR spectra at the joining interface (Fig. 15). All these studies further demonstrate that the presence of carbonyl group (C=O) is critically important to achieving a strong chemical bonding between metal and polymer substrates.

Functional Group Seeding

Non-polar polymers (i.e., polymers without functional groups in their chemical structure) are not capable of directly forming chemical bonds at the metal-polymer interface (Refs. 20, 101–105). One cost-effective solution was to introduce functional group seeding either in-situ or ex-situ. Along this line, Liu et al. (Refs. 48, 106) have recently proposed that 3D distributed chemical bonds (3D ChemBonds) can be produced in-situ between metal and polymer through trapped air pockets at the joint interface. These air pockets induce the necessary carbonyl groups in the inert polymer which in turn helps form the chemical bond observed.

Khan et al. (Ref. 21) recently developed a simple and effective functional group seeding method via using a readily available PA6 thin film between aluminum alloy and PP composite to enable the metal-PP composite joining under a friction-based joining process, as illustrated in Fig. 16. This technique is shown working well for polymer composites with inert polymer resins and any combination of reinforced fibers. Once the seeding material is placed between the metal and

the inert polymer composite sheets, suitable conditions of temperature and pressure need to be imposed to melt both polymers and formulate an intermixed multi-material fiber composite at the interface. Using an off-the-shelf 50 µm thin PA6 film not only the joining was enabled between aluminum alloy and GFRP-PP composite (Fig. 17), but the load-bearing capability was also maximized such that the joint did not fail under the lap shear tensile condition, rather, the base GFRP-PP material failed at the bulk material through-thickness (Fig. 17).

Their investigations showed that the joint interface between PP and aluminum alloy was intimately bonded through the thin PA6 intermediate layer forming an intermixed composite network among the available glass fibers and the PP matrix (Fig. 18). A closer look at the Al-PA interface (Fig. 18) revealed that the joining interface is indistinguishable at a 200 nm length scale suggesting strong possibility of chemical or molecular level bonding at the joint interface between Al and PA materials.

Bonding and Joint Strength Enhancement Methods

Although direct chemical bonding between metal and polymer substrates can be achieved if inherent functional groups are present in the polymers (polar polymers such as PA or PC), for engineering applications, additional measures for ensuring sufficient joint strength are required. This is because chemical reaction sites at a joint interface can be limited or nonuniformly distributed, due to process variability. There are numerous metals or polymer surface or bulk material pre-treatment techniques being reported in the literature, as briefly highlighted below.
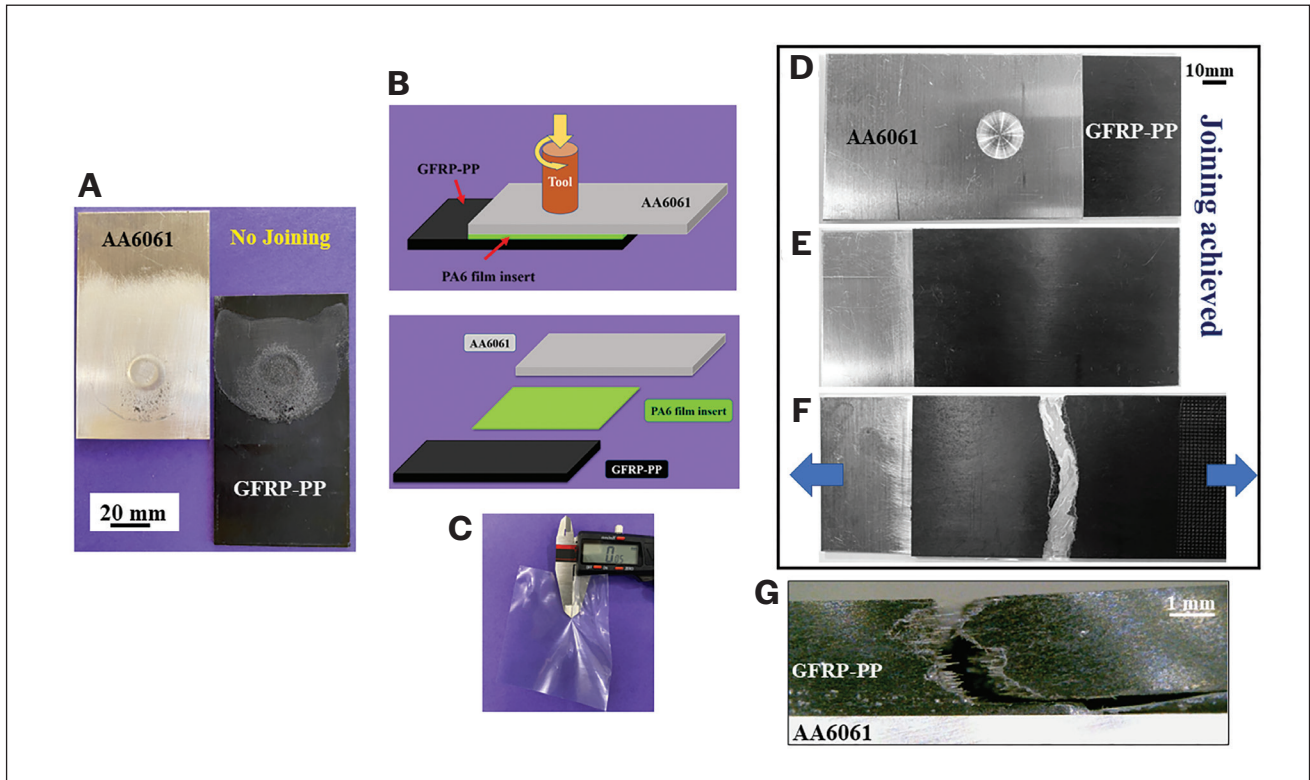
Fig. 17 — Al-GFPP joint formation using functional group seeding and substrate failure (Ref. 21).
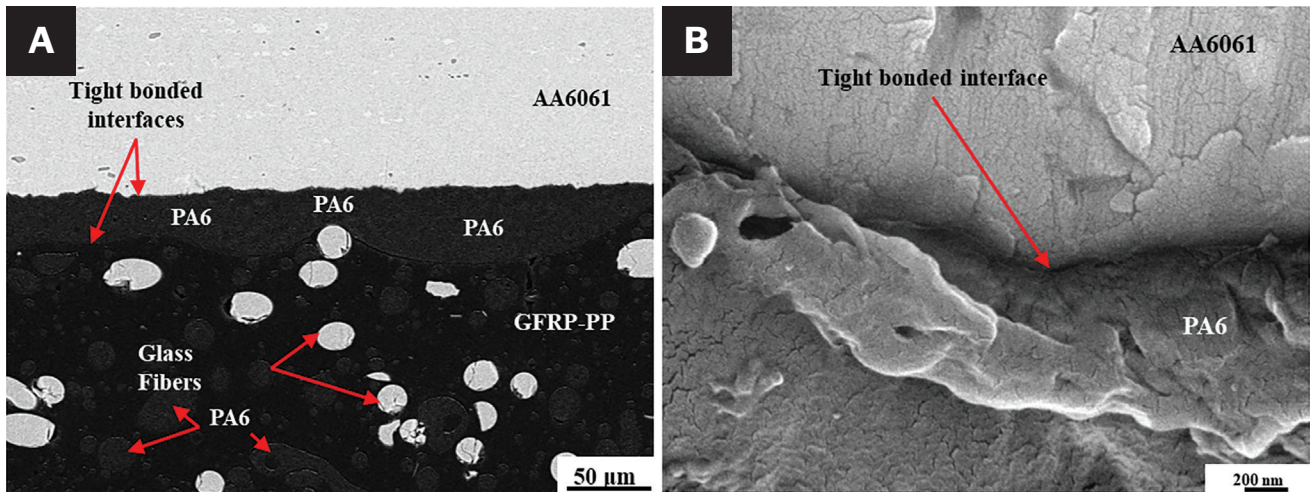
Fig. 18 — Bonding interface in Al-GFPP joints (Ref. 21).

Metal Pre-Treatment

Metal pre-treatment can be used to generate mechanical features at various length scales to assist and increase mechanical interlocking effects (Refs. 110–115). When performed at micro or nano scale (Refs. 116–119), this also increases the surface energy of the metal surface and provides higher wettability. Laser texturing (Fig. 19A) has been efficient in developing mechanical grooves to provide an anchoring effect and increase joining between metal and polymers (Refs. 22, 120–122). A sequence of chemical etching using sodium hydroxide (NaOH), hydrochloric acid (HCl), and hydrazine (N2H4) is another way to locally dissolve metal surfaces (usually soft metals such as aluminum alloys) and generate nanopores (Fig. 19B) to assist seeping in the polymer melt and form micro-mechanical interlocking effects (Ref. 107). Electrochemical etching (surface anodizing) has also been an effective method to generate a controlled honeycomb morphology (Fig. 19C) on aluminum alloys for joining with non-polar polymers (Refs. 108, 123–125). Alternatively, silane-type chemical coupling agents (Refs. 126–128) and plasma electrolytic oxidation (Refs. 129, 130) can be used
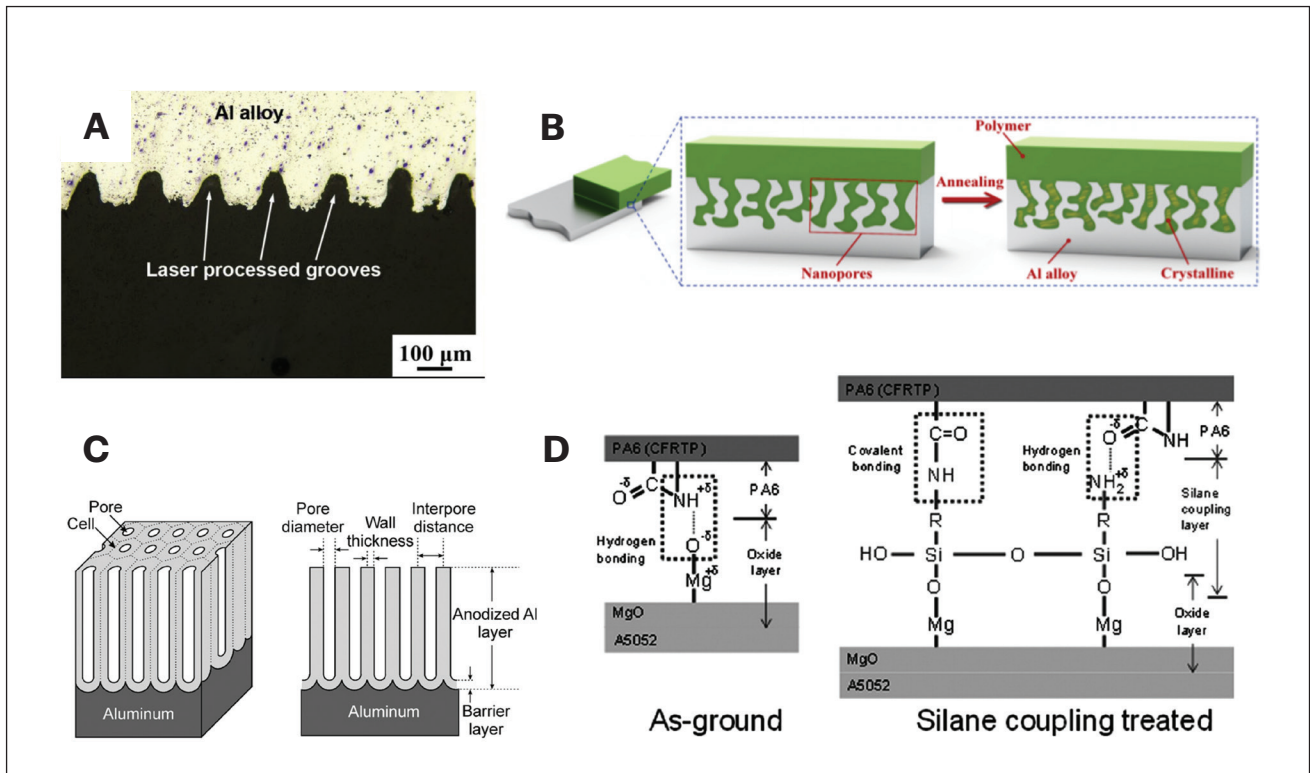
Fig. 19 — Metal surface pre-treatment methods: A — Laser texturing on the metal surface (Ref. 22); B — chemical etching method to generate micro mechanical anchoring effect (Ref. 107); C — surface anodization in aluminum to provide honeycomb pores (Ref. 108); D — mechanism of silane coupling (Ref. 109).
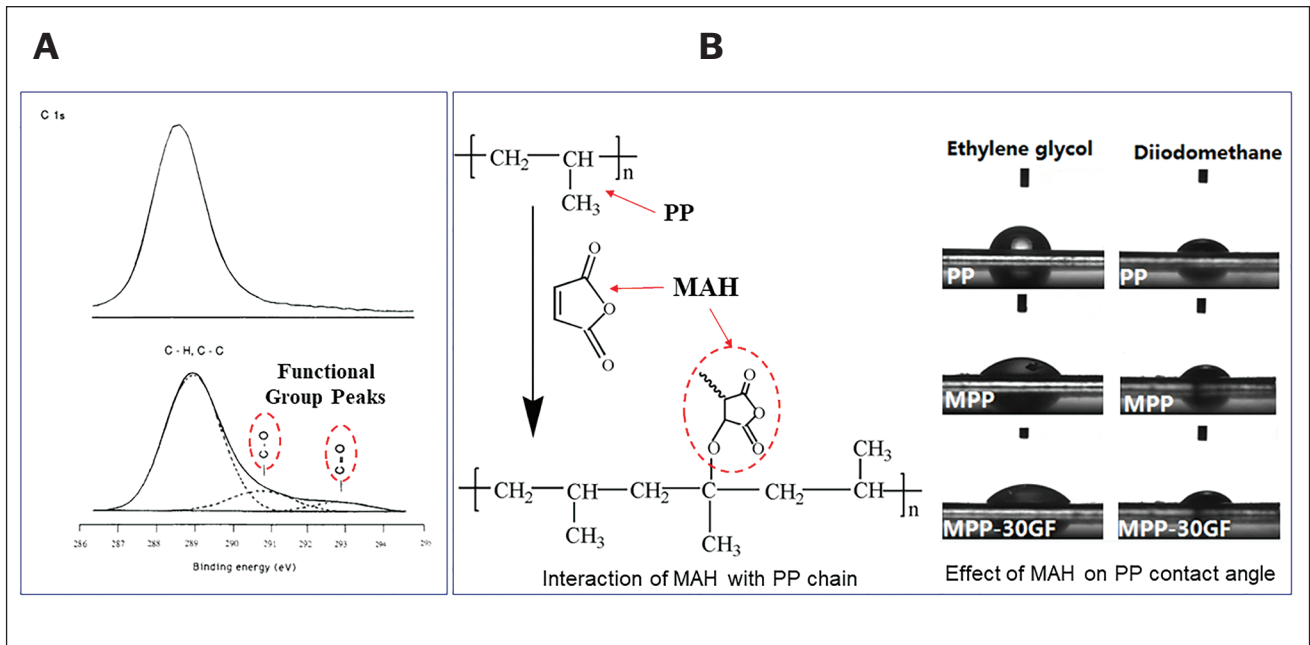
Fig. 20 — Polymer pre-treatment methods: A — Effect of plasma treatment on PP surface conditions (Ref. 131); B — effect of MAH grafting on PP (Ref. 132).

on the metal surface when mechanical anchoring features are not desirable. Silane is a chemical coupling agent with multiple carbonyl (C=O) type functional groups. Due to its strong polar nature (Fig. 19D), it reacts with the metal surface (or native oxide when available) to form strong linkages between the metal and the polymer joining partners. For example, it generates chemical reaction sites by formulating a covalent bonding in addition to the proposed hydrogen bonding compared to the untreated condition (Fig. 19D) when joining aluminum alloy with PA6 (Ref. 109).

Polymer Pre-Treatment

Other than micro-mechanical interlocking methods, the polymer side can be treated either on the surface or in a bulk manner (Refs. 133–137). These processes share the same principle of either inducing or providing functional groups (C=O) on the surface or in the bulk of the polymer matrix and are called polymer functionalization. For example, using controlled atmospheric and inert vacuum plasma treatments distinguishable carbonyl groups (C=O) can be generated on the PP surface (confirmed by XPS in Fig. 20A) (Refs. 104, 131, 138–140). On the other hand, bulk grafting of PP using anhydride has also proven vital to functionalize PP and enable joining with metal counterparts (Refs. 141–145). Maleic anhydride (MAH) is one of the most used grafting compounds which contains multiple carbonyl type (C=O) functional groups in its cyclic chemical structure (Fig. 20B). Untreated PP can be used in small pellets in a blend with MAH and the blend can be co-extruded to form a modified grafted PP (MAH-g-PP) below the decomposition temperature of PP. Carbonyl-type functional groups thus can be grafted in the PP and the surface energy of such grafted-PP increases (Refs. 101, 137, 146). Surface energy increase and introduction of functional groups make it possible for grafted PP to react chemically with the metal joining partner under the prescribed localized heat and pressure conditions.

Limitations of Bonding Enhancement Methods

Most surface treatment methods discussed above are still cost and time-prohibitive for use in mass production environments. For instance, mechanical or physical surface modification of the metal side is time-consuming. The resulting mechanical protrusions tend to serve stress concentration sites in structural applications. Chemical bulk structure modification or chemical surface treatment on the polymer side involves various steps to be followed to achieve a reasonable bonding strength in metal polymer hybrid (MPH) joints. The process of functionalizing non-functional (non-polar) polymers generates a very thin layer of such carbonyl groups, usually of a few hundred nanometers, and requires immediate joining operation before degradation occurs. This can be a major limitation for its use in a production environment.

Concluding Remarks

A state-of-the-art assessment of polymer-metal joining research and promising techniques have been presented, with a particular emphasis on their potential for structural applications in the mass-produced marketplace. Direct welding of polymer to metal is not only possible but also shows the potential for applications in mass-production environments, in addition to its simplicity and excellent joint performance for some dissimilar material combinations. To accelerate a broad adoption of this novel joining technique for supporting the industry's drive towards multi-material lightweighting, three major hurdles need to be overcome. These are; (1) an improved understanding of C-O-M chemical bond development mechanisms and their controlling parameters; (2) effective procedures for extracting joint properties from simple lab test specimens for supporting computer-aided engineering of multi-material structures; and (3) joint design guidelines for improved jointability in process and joint performance in structural context.

Regarding the C-O-M chemical bond mechanisms, the carbonyl functional group (C=O) has been the most important chemical component for achieving the strong direct joining between the metals and the polymers (plastic). However, there are multiple theories on the bond formation mechanisms. Al-O-C type covalent bond formation between the aluminum and the polymer chain via carbonyl group, covalent bond formation between native aluminum oxide and the polymeric chain, and hydrogen bonding between the native aluminum oxide and the polymeric chain via hydrolysis of hydrocarbons in conjunction with the carbonyl group is among the top. The Van der Waals effect at the bonding interface is also considered a contributing factor. How to experimentally confirm one dominant bonding mechanism and to what extent over others under a given direct joining process condition remains challenging. The ability to do so is important for developing an optimized direct joining process for promoting the uniformity and sufficient length scale of the resulting covalent chemical bond. In addition to capable measurement and characterization techniques, novel experimental approaches to isolate and promote the bonding mechanisms can be effective for elucidating a favorable bond formation environment. Such insights played a key role in their subsequent process development.

With an improved understanding of the C-O-M bonding mechanisms and the chemical bond quality improvement techniques reviewed in this article, some mainsteam structural applications are expected to be realized shortly for achieving ever-increasingly structural lightweight goals by the transportation industry.

References

1. Lamb, W. F., Wiedmann, T., Pongratz, J., Andrew, R., Crippa, M., and Olivier, J. G. J., et al. 2021. A review of trends and drivers of greenhouse gas emissions by sector from 1990 to 2018. *Environmental Research Letters* 16. DOI: 10.1088/1748-9326/abee4e

2. Keoleian, G. A., and Sullivan, J. L. 2012. Materials challenges and opportunities for enhancing the sustainability of automobiles. *MRS Bulletin* 37: 365–72. DOI: 10.1557/mrs.2012.52

3. Kelly, J. C., Sullivan, J. L., Burnham, A., and Elgowainy, A. 2015. Impacts of vehicle weight reduction via material substitution on life-cycle greenhouse gas emissions. *Environmental Science and Technology* 49: 12535–42. DOI: 10.1021/acs.est.5b03192

4. Taub, A., De Moor, E., Luo, A., Matlock, D. K., Speer, J. G., and Vaidya, U. 2019. Materials for automotive lightweighting. *Annual Review of Materials Research* 49: 327–59. DOI: 10.1146/annurev-matsci-070218-010134

5. Goede, M., Stehlin, M., Rafflenbeul, L., Kopp, G., and Beeh, E. 2009. Super light car—Lightweight construction thanks to a multi-material design and function integration. *European Transport Research Review* 1: 5–10.

6. Hürkamp, A., Dér, A., Gellrich, S., Ossowski, T., Lorenz, R., and Behrens, B-A, et al. 2020. Integrated computational product and production engineering for multi-material lightweight structures. *International Journal of Advanced Manufacturing Technology* 110: 2551–71.

7. Meschut, G., Janzen, V., and Olfermann, T. 2014. Innovative and highly productive joining technologies for multi-material lightweight car body structures. *Journal of Materials Engineering and Performance* 23: 1515–23.

8. Dong, P. Quantitative weld quality acceptance criteria: An enabler for structural lightweighting and additive manufacturing. *Welding Journal* 99(2): 39-51. DOI: 10.29391/2020.99.004

9. Conklin, J., Beals, R., and Brown, Z. 2015. BIW design and CAE MMLV lightweight body in white structure multi material lightweight vehicle (MMLV). *SAE International.* DOI: 10.4271/2015-01-0408

10. Jaranson, J. and Ahmed, M. 2015. MMLV: lightweight interior systems design. *SAE International.* DOI: 10.4271/2015-01-1236

11. Blanco, D., Rubio, E. M., Marín, M. M., and Davim, J. P. 2021. Advanced materials and multi-materials applied in aeronautical and automotive fields: A systematic review approach. *Procedia CIRP* 99: 196–201. DOI: 10.1016/j.procir.2021.03.027

12. Martinsen, K., Hu, S. J., and Carlson, B. E. 2015. Joining of dissimilar materials. *CIRP Annals* 64:679–99. DOI: 10.1016/j.cirp.2015.05.006

13. Skszek, T. and Conklin, J. 2015. Multi-material lightweight vehicle acknowledgment. *U.S. Department of Energy.*

14. Pramanik, A., Basak, A. K., Dong, Y., Sarker, P. K., Uddin, M. S., and Littlefair, G., et al. 2017. Joining of carbon fibre reinforced polymer (CFRP) composites and aluminium alloys – A review. *Composites Part A: Applied Science and Manufacturing* 101: 1–29. DOI: 10.1016/j.compositesa.2017.06.007

15. Galińska, A. 2020. Mechanical joining of fibre reinforced polymer composites to metals—A review. Part 1: Bolted joining. *Polymers* 12(10). DOI: 10.3390/polym12102252

16. Lißner, M., Erice, B., Alabort, E., Thomson, D., Cui, H., and Kaboglu, C., et al. Multi-material adhesively bonded structures: Characterisation and modelling of their rate-dependent performance. *Composites Part B: Engineering* 195:108077. DOI: 10.1016/j.compositesb.2020.108077

17. Lambiase, F., Balle, F., Blaga, L. A., Liu, F., and Amancio-Filho, S. T. 2021. Friction-based processes for hybrid multi-material joining. *Composites Structures* 266: 113828. DOI: 10.1016/J.COMPSTRUCT.2021.113828

18. Lambiase, F., Scipioni, S. I., Lee, C. J., Ko, D. C., and Liu, F. 2021. A state-of-the-art review on advanced joining processes for metal-composite and metal-polymer hybrid structures. *Materials* 14. DOI: 10.3390/ma14081890

19. Lambiase, F., and Liu, F. 2021. Recent advances in metal-polymer joining processes. *Joining Processes for Dissimilar and Advanced Materials*. DOI: 10.1016/B978-0-323-85399-6.00007-2

20. Liu, F. C., Dong, P., Lu, W., and Sun, K. 2019. On formation of AlOC bonds at aluminum/polyamide joint interface. *Applied Surface Science* 466: 202–9. DOI: 10.1016/j.apsusc.2018.10.024

21. Khan A. S., Liu, F., and Dong, P. 2023. Joining of metal and non-polar polypropylene composite through a simple functional group seeding layer. *Journal of Manufacturing Processes* 85: 90–100. DOI: 10.1016/J.JMAPRO.2022.11.022

22. Han, S. C., Wu, L. H., Jiang, C. Y., Li, N., Jia, C. L., and Xue, P., et al. 2020. Achieving a strong polypropylene/aluminum alloy friction spot joint via a surface laser processing pretreatment. *Journals of Materials Science & Technology* 50: 103–14. DOI: 10.1016/j.jmst.2020.02.035

23. Kawahito, Y., Tange, A., Kubota, S., and Katayama, S. 2006. Development of direct laser joining for metal and plastic. *Pacific International Conference on Applications of Lasers and Optics* 604. DOI: 10.2351/1.5060840

24. Shang, S. L., Sun, H., Pan, B., Wang, Y., Krajewski, A. M., and Banu, M., et al. 2021. Forming mechanism of equilibrium and non-equilibrium metallurgical phases in dissimilar aluminum/steel (Al-Fe) joints. *Scientific Reports* 11: 24251.

25. Watanabe, M., Feng, K., Nakamura, Y., and Kumai, S. Growth manner of intermetallic compound layer produced at welding interface of friction stir spot welded aluminum/steel lap joint. *Materials Transactions* 52: 953–9. DOI: 10.2320/matertrans.L-MZ201120

26. Wang, K., Shang, S. L., Wang, Y., Vivek, A., Daehn, G., and Liu, Z-K. et al. 2020. Unveiling non-equilibrium metallurgical phases in dissimilar Al-Cu joints processed by vaporizing foil actuator welding. *Materials & Design* 186: 108306.

27. Liu, F. C., and Dong, P. 2021. From thick intermetallic to nanoscale amorphous phase at Al-Fe joint interface: Roles of friction stir welding conditions. *Scripta Materialia* 191: 167–72. DOI: 10.1016/j.scriptamat.2020.09.031

28. Liu, F. C., Dong, P., Khan, A. S., Sun, K., Lu, W., and Taub A., et al. 2022. Amorphous interfacial microstructure and high bonding strength in Al-Fe bimetallic components enabled by a large-area solid-state additive manufacturing technique. *Journal of Materials Processing Technology* 308: 117721. DOI: 10.1016/J.JMATPROTEC.2022.117721

29. Liu, F. C., Dong, P., Zhang, J., Lu, W., Taub, A., and Sun, K. 2020. Alloy amorphization through nanoscale shear localization at Al-Fe interface. *Materials Today Physics* 15(2): 100252. DOI: 10.1016/j.mtphys.2020.100252

30. Liu, F., Zhang, Y., and Dong, P. 2022. Large area friction stir additive manufacturing of intermetallic-free aluminum-steel bimetallic components through interfacial amorphization. *Journal of Manufacturing Processes* 73: 725–35. DOI: 10.1016/j.jmapro.2021.11.042

31. Friedrich, K. 2016. Carbon fiber reinforced thermoplastic composites for future automotive applications. *AIP Conference Proceedings* 1736. DOI: 10.1063/1.4949575

32. Holbery, J., and Houston, D. 2006. Natural-fiber-reinforced polymer composites in automotive applications. *JOM* 58: 80–6. DOI: 10.1007/s11837-006-0234-2

33. Elmarakbi, A. 2013. *Advanced composite materials for automotive applications: Structural integrity and crashworthiness*. John Wiley & Sons.

34. Stewart, R. 2011. Thermoplastic composites - Recyclable and fast to process. *Reinforced Plastics* 55: 22–8. DOI: 10.1016/S0034-3617(11)70073-X

35. Bel Haj Frej, H., Léger, R., Perrin, D., and Ienny, P. 2021. A novel thermoplastic composite for marine applications: Comparison of the effects of aging on mechanical properties and diffusion mechanisms. *Applied Composite Materials* 28(4): 899–922. DOI: 10.1007/s10443-021-09903-0

36. Shanmugam, L., Kazemi, M. E., Rao, Z., Yang, L., and Yang, J. 2020. On the metal thermoplastic composite interface of Ti alloy/UHMWPE-Elium® laminates. *Composites Part B: Engineering* 181: 107578. DOI: 10.1016/j.compositesb.2019.107578

37. da Costa, A. P., Botelho, E. C., Costa, M. L., Narita, N. E., and Tarpani, J. R. 2012. A review of welding technologies for thermoplastic composites in aerospace applications. *Journal of Aerospace Technology and Management* 4(3): 255–65. DOI: 10.5028/jatm.2012.04033912

38. Roux, M., Dransfeld, C., Eguémann, N., and Giger, L. 2014. Processing and recycling of a thermoplastic composite fibre/peek aerospace part. *16th European Conference on Composite Material*: 22–6.

39. Wagner, D., Conklin, J. L., Zaluzec, M., and Skszek, T. W. 2015. *The multi material lightweight vehicle (MMLV) project*. SAE International.

40. Pradeep, S. A., Iyer, R. K., Kazan, H., and Pilla, S. 2017. Automotive applications of plastics: Past, present, and future. *Applied Plastics Engineering Handbook*: 651–673. DOI: 10.1016/B978-0-323-39040-8.00031-6

41. Patil, A., Patel, A., and Purohit, R. 2017. An overview of polymeric materials for automotive applications. *Materials Today Proceedings* 4(2): 3807–15. DOI: 10.1016/j.matpr.2017.02.278

42. Mallick, P. K. 2020. Thermoplastics and thermoplastic–matrix composites for lightweight automotive structures. *Materials, Design and Manufacturing for Lightweight Vehicles*. DOI: 10.1016/B978-0-12-818712-8.00005-7

43. Foss, P. H., Mentzer, C. C., and Franklin, D. W. 2004. Design and valifation of a thermoplastic composite liftgate. Glass.

44. Maddah, H. A. 2016. Polypropylene as a promising plastic: A review. *American Journal of Polymer Science*. DOI: 10.5923/j.ajps.20160601.01

45. Lorenzo, L., and Naughton, P. 2002. Structural front-end carrier using long glass fiber polypropylene. *SAE Technical Paper*. DOI: 10.4271/2002-01-3563

46. Hariprasad, K., Ravichandran, K., Jayaseelan, V., and Muthuramalingam, T. 2020. Acoustic and mechanical characterisation of polypropylene composites reinforced by natural fibres for automotive applications. *Journal of Materials Research and Technology* 9: 14029–35. DOI: 10.1016/j.jmrt.2020.09.112

47. Burn, D. T. 2016. Long discontinuous carbon fibre/polypropylene composites for high volume automotive applications. University of Nottingham.

48. Liu F., and Dong, P. 2022. Directly and Reliably Welding Plastic to Metal. *Welding Journal* 101:45–8.

49. Staab, F., Liesegang, M., and Balle, F. 2020. Local shear strength distribution of ultrasonically welded hybrid aluminium to CFRP joints. *Composite Structures* 248: 112481. DOI: 10.1016/j.compstruct.2020.112481

50. Staab, F. and Balle, F. 2022. Fatigue and fracture of ultrasonically welded aluminum alloys to carbon fiber reinforced thermoplastics. *Fatigue & Fracture Engineering Materials & Structures* 45: 607–16. DOI: 10.1111/ffe.13622

51. Wagner, D. 2015. Multi Material Lightweight Vehicle (MMLV) Architecture. *U.S. Department of Energy*.

52. Kleinbaum, S., Jiang, C., and Logan, S. 2019. Enabling sustainable transportation through joining of dissimilar lightweight materials. *MRS Bulletin* 44: 608–12. DOI: 10.1557/mrs.2019.178

53. Khayoon, M. A., Hubeatir, K. A., and Al-Khafaji, M. M. 1973. Laser transmission welding is a promising joining technology technique–A recent review. *Journal of Physics Conference Series* 1: 012023. DOI: 10.1088/1742-6596/1973/1/012023

54. Huang, Y., Gao, X., Zhang, Y., and Ma, B. 2022. Laser joining technology of polymer-metal hybrid structures – A review.

Journal of Manufacturing Processes 79: 934–61. DOI: 10.1016/j.jmapro.2022.05.026

55. Jiao, J., Xu, Z., Wang, Q., Sheng, L., and Zhang, W. 2018. CFRTP and stainless steel laser joining: Thermal defects analysis and joining parameters optimization. *Optics & Laser Technology* 103:170–6. DOI: 10.1016/j.optlastec.2018.01.023

56. Su, J., Tan, C., Wu, Z., Wu, L., Gong, X., and Chen, B., et al. 2020. Influence of defocus distance on laser joining of CFRP to titanium alloy. *Optics and Laser Technology* 124:106006. DOI: 10.1016/j.optlastec.2019.106006

57. Huang, Y., Gao, X., Ma, B., and Zhang, Y. 2021. Interface formation and bonding mechanisms of laser welding of PMMA plastic and 304 austenitic stainless steel. *Metals* 11(9): 1495. DOI: 10.3390/met11091495

58. Wang, H., Xiao, X., Xiao, G., Fan, H-T., and Arinez, J. 2019. Laser joining of carbon-fiber-reinforced polymer and metal with high-strength and corrosion-resistant bonds. *Procedia Manufacturing* 34: 42–8. DOI: 10.1016/j.promfg.2019.06.112

59. Jung, K. W., Kawahito, Y., Takahashi, M., and Katayama, S. 2013. Laser direct joining of carbon fiber reinforced plastic to aluminum alloy. *Journal of Laser Applications* 25: 032003. DOI: 10.2351/1.4794297

60. Jung, K. W., Kawahito, Y., Takahashi, M., and Katayama, S. 2013. Laser direct joining of carbon fiber reinforced plastic to zinc-coated steel. *Materials & Design* 47: 179–88. DOI: 10.1016/j.matdes.2012.12.015

61. Rodríguez-Vidal, E., Lambarri, J., Soriano, C., Sanz, C., and Verhaeghe, G. 2014. A combined experimental and numerical approach to the laser joining of hybrid polymer – Metal parts. *Physics Procedia* 56: 835–44. DOI: 10.1016/j.phpro.2014.08.101

62. Tamrin, K. F., Nukman, Y., and Zakariyah, S. S. 2013. Laser lap joining of dissimilar materials: A review of factors affecting joint strength. *Materials and Manufacturing Processes* 28: 857–71. DOI: 10.1080/10426914.2013.792413

63. Tillmann, W., Elrefaey, A., and Wojarski, L. 2010. Toward process optimization in laser welding of metal to polymer. *Materials Science & Engineering Technology* 41: 879–83. DOI: 10.1002/mawe.201000674

64. Farazila, Y., Miyashita, Y., Hua, W., Mutoh, Y., and Otsuka, Y. 2011. YAG Laser spot welding of PET and metallic materials. *Journal of Laser Micro/Nanoengineering* 6(1). DOI: 10.2961/jlmn.2011.01.0015

65. Miyashita, Y., Takahashi, M., Takemi, M., Oyama, K., Mutoh, Y., and Tanaka H. 2009. Dissimilar materials micro welding between stainless steel and plastics by using pulse yag laser. *Journal of Solid Mechanics and Materials Engineering* 3: 409–15. DOI: 10.1299/jmmp.3.409

66. Rodríguez-Vidal, E., Sanz, C., Lambarri, J., Renard, J., and Gantchenko, V. 2016. Laser joining of different polymer-metal configurations: Analysis of mechanical performance and failure mechanisms. *Physics Procedia* 83: 1110–7. DOI: 10.1016/j.phpro.2016.09.002

67. Murzin, S. P., Palkowski, H., Melnikov, A. A., and Blokhin, M. V. 2022. Laser welding of metal-polymer-metal sandwich panels. *Metals* 12. DOI: 10.3390/met12020256

68. Borba, N. Z. 2018. Use of CFRP composites and new joining processes in aircraft fuselage.

69. Liu, F. C., and Ma, Z. Y. 2008. Influence of tool dimension and welding parameters on microstructure and mechanical properties of friction-stir-welded 6061-T651 aluminum alloy. *Metallurgical Materials Transactions A* 39: 2378–88. DOI: 10.1007/s11661-008-9586-2

70. Ma, N., Geng, P., Ma, Y., Shimakawa, K., Choi, J. W., and Aoki, Y., et al. 2021. Thermo-mechanical modeling and analysis of friction spot joining of Al alloy and carbon fiber-reinforced polymer. *Journal*

of Materials Research and Technology 12: 1777–93. DOI: 10.1016/j.jmrt.2021.03.111

71. Amancio-Filho, S. T., Bueno, C., dos Santos, J. F., Huber, N., and Hage, E. 2011. On the feasibility of friction spot joining in magnesium/fiber-reinforced polymer composite hybrid structures. *Materials Science and Engineering: A* 528: 3841–8. DOI: 10.1016/j.msea.2011.01.085

72. Liu, F. C., Liao, J., and Nakata, K. 2014. Joining of metal to plastic using friction lap welding. *Materials & Design* 54: 236–44. DOI: 10.1016/j.matdes.2013.08.056

73. Liu, F. C., Nakata, K., Liao, J., Hirota, S., and Fukui, H. 2014. Reducing bubbles in friction lap welded joint of magnesium alloy and polyamide. *Science and Technology Welding Joining* 19: 578–87. DOI: 10.1179/1362171814Y.0000000228

74. Lambiase, F., Grossi, V., Scipioni, S. I., and Paoletti, A. 2021. Prediction of the power supplied in friction-based joining process of metal-polymer hybrids through machine learning. *Journal of Manufacturing Processes* 68: 750–60. DOI: 10.1016/J.JMAPRO.2021.06.001

75. Tan, X., Zhang, J., Shan, J., Yang, S., and Ren, J. 2015. Characteristics and formation mechanism of porosities in CFRP during laser joining of CFRP and steel. *Composites Part B: Engineering* 70: 35–43. DOI: 10.1016/j.compositesb.2014.10.023

76. Liu, F. C., Dong, P., and Pei, X. A high-speed metal-to-polymer direct joining technique and underlying bonding mechanisms. *Journal of Materials Processing Technology* 280: 116610. DOI: 10.1016/j.jmatprotec.2020.116610

77. Goushegir, S. M., dos Santos, J. F., and Amancio-Filho, S. T. 2014. Friction Spot Joining of aluminum AA2024/carbon-fiber reinforced poly(phenylene sulfide) composite single lap joints: Microstructure and mechanical performance. *Materials & Design* 54: 196–206. DOI: 10.1016/j.matdes.2013.08.034

78. Liu, F. C., Dong, P., and Pei, X. A high-speed metal-to-polymer direct joining technique and underlying bonding mechanisms. *Journal of Materials Processing Technology* 280: 116610. DOI: 10.1016/j.jmatprotec.2020.116610

79. McIntyre, D. 2015. Characterisation. *The Cambridge Handbook of Stylistics*. DOI: 10.1017/CBO9781139237031.013

80. Bauernhuber, A., Markovits, T., Trif, L., and Csanády Á. 2017. Adhesion of steel and PMMA by means of laser radiation. *Materials Science Forum* 885: 61–6. DOI: 10.4028/www.scientific.net/MSF.885.61

81. Csiszér, T., Temesi, T., Borbás, L., and Molnár, L. 2021. Laser-assisted joining of steel and cellulose fiber-reinforced pmma. *Acta Polytech Hungarica* 18: 237–53. DOI: 10.12700/APH.18.2.2021.2.13

82. Hussein, F. I., Akman, E., Genc Oztoprak, B., Gunes, M., Gundogdu, O., and Kacar, E., et al. 2013. Evaluation of PMMA joining to stainless steel 304 using pulsed Nd:YAG laser. *Optics & Laser Technology* 49: 143–52. DOI: 10.1016/j.optlastec.2012.12.028

83. Barakat, A. A., Darras, B. M., Nazzal, M. A., and Ahmed, A. A. 2023. A comprehensive technical review of the friction stir welding of metal-to-polymer hybrid structures. *Polymers* 15(1): 220. DOI: 10.3390/polym15010220

84. Meiabadi, M. S. S. M., Kazerooni, A., Moradi, M., and Torkamany, M. J. 2020. Laser assisted joining of St12 to polycarbonate: Experimental study and numerical simulation. *Optik* 208: 164151. DOI: 10.1016/j.ijleo.2019.164151

85. Ai, Y., Zheng, K., Shin, Y. C., and Wu, B. 2018. Analysis of weld geometry and liquid flow in laser transmission welding between polyethylene terephthalate (PET) and Ti6Al4V based on numerical simulation. *Optics & Laser Technology* 103: 99–108. DOI: 10.1016/j.optlastec.2018.01.022

86. Chan, C. W., and Smith, G. C. 2016. Fibre laser joining of highly dissimilar materials: Commercially pure Ti and PET hybrid joint for medical device applications. *Materials & Design* 103: 278–92. DOI: 10.1016/j.matdes.2016.04.086

87. Wahba, M., Kawahito, Y., and Katayama, S. 2011. Laser direct joining of AZ91D thixomolded Mg alloy and amorphous polyethylene terephthalate. *Journal of Materials Processing Technology* 211: 1166–74. DOI: 10.1016/j.jmatprotec.2011.01.021

88. Yusof, F., Miyashita, Y., Seo, N., Mutoh, Y., and Moshwan, R. 2012. Utilising friction spot joining for dissimilar joint between aluminium alloy (A5052) and polyethylene terephthalate. *Science Technology of Welding and Joining* 17: 544–9. DOI: 10.1179/13621 7112x13408696326530

89. Balle, F., Wagner, G., and Eifler, D. 2009. Ultrasonic metal welding of aluminium sheets to carbon fibre reinforced thermoplastic composites. *Advanced Engineering Materials* 11: 35–9. DOI: 10.1002/adem.200800271

90. Jung, K. W., Kawahito, Y., and Katayama, S. 2011. Laser direct joining of carbon fibre reinforced plastic to stainless steel. *Science and Technology of Welding and Joining* 16: 676–80. DOI: 10.1179/1362171811Y.0000000060

91. Nagatsuka, K., Kitagawa, D., Yamaoka, H., and Nakata, K. 2016. Friction lap joining of thermoplastic materials to carbon steel. *ISIJ International* 56: 1226–31. DOI: 10.2355/isijinternational.ISIJINT-2016-042

92. Lambiase, F., and Paoletti, A. 2018. Mechanical behavior of AA5053/polyetheretherketone (PEEK) made by friction assisted joining. *Composites Structures* 189: 70–8. DOI: 10.1016/j.compstruct.2018.01.045

93. Tao, W., Su, X., Chen, Y., and Tian, Z. 2019. Joint formation and fracture characteristics of laser welded CFRP/TC4 joints. *Journal of Manufacturing Processes* 45: 1–8. DOI: 10.1016/j.jmapro.2019.05.028

94. Ageorges, C., and Ye, L. 2001. Resistance welding of metal/thermoplastic composite joints. *Journal of Thermoplastic Composite Materials* 14: 449–75. DOI: 10.1106/PN74-QXKH-7XBE-XKF5

95. Feistauer, E. E., Guimarães, R. P. M., Ebel, T., dos Santos, J. F., and Amancio-Filho, S. T. 2016. Ultrasonic joining: A novel direct-assembly technique for metal-composite hybrid structures. *Materials Letters* 170: 1–4. DOI: 10.1016/j.matlet.2016.01.137

96. Gao, T., et al. An Internal Res Report, University of Michigan.

97. Zhao, S., Kimura, F., Wang, S., and Kajihara, Y. 2021. Chemical interaction at the interface of metal–Plastic direct joints fabricated via injection molded direct joining. *Applied Surface Science* 540: 148339. DOI: 10.1016/j.apsusc.2020.148339

98. Arenas, J. M., Alía, C., Narbón, J. J., Ocaña, R., and González, C. 2013. Considerations for the industrial application of structural adhesive joints in the aluminium–composite material bonding. *Composites Part B: Engineering* 44: 417–23. DOI: 10.1016/j.compositesb.2012.04.026

99. Pletincx, S., Fockaert, L. L. I., Mol, J. M. C., Hauffman, T., and Terryn, H. 2019. Probing the formation and degradation of chemical interactions from model molecule/metal oxide to buried polymer/metal oxide interfaces. *Npj Materials Degradation* 3: 1–12. DOI: 10.1038/s41529-019-0085-2

100. Hirchenhahn, P., Al Sayyad, A., Bardon, J., Felten, A., Plapper, P., and Houssiau, L. 2020. Highlighting chemical bonding between nylon-6.6 and the native oxide from an aluminum sheet assembled by laser welding. *ACS Applied Polymer Materials* 2: 2517–27. DOI: 10.1021/acsapm.0c00015

101. Liu, Y., Shigemoto, Y., Hanada, T., Miyamae, T., Kawasaki, K., and Horiuchi, S. 2021. Role of chemical functionality in the adhesion of aluminum and isotactic polypropylene. *ACS Applied Materials & Interfaces* 13: 11497–506. DOI: 10.1021/acsami.0c22988

102. Ochoa-Putman, C., and Vaidya, U. K. 2011. Mechanisms of interfacial adhesion in metal–polymer composites – Effect of chemical treatment. *Composite Part A: Applied Science Manufacturing* 42: 906–15. DOI: 10.1016/j.compositesa.2011.03.019

103. Ramarathnam, G., Libertucci, M., Sadowski, M., and North, T. 1992. Joining of polymers to metal. *Welding Journal* 71: 483-s.

104. Mandolfino, C., Lertora, E., Gambaro, C., and Pizzorni, M. 2019. Functionalization of neutral polypropylene by using low pressure plasma treatment: Effects on surface characteristics and adhesion properties. *Polymers* 11. DOI: 10.3390/polym11020202

105. Melentiev, R., Yudhanto, A., Tao, R., Vuchkov, T., and Lubineau, G. 2022. Metallization of polymers and composites: State-of-the-art approaches. *Materials & Design* 221: 110958. DOI: 10.1016/J.MATDES.2022.110958

106. Liu F, and Dong P. 2023. A high-speed polymer-to-metal direct joining system and method.

107. Xie, Y., Zhang, J., and Zhou, T. 2019. Large-area mechanical interlocking via nanopores: Ultra-high-strength direct bonding of polymer and metal materials. *Applied Surface Science* 492: 558–70. DOI: 10.1016/j.apsusc.2019.06.246

108. Sulka, G. D. 2008. Highly ordered anodic porous alumina formation by self-organized anodizing. *Nanostructured Materials in Electrochemistry*: 1–116. DOI: 10.1002/9783527621507

109. Kimiaki, N., Hironobu, T., Bolyu, X., Atsuki, T., and Kazuhiro, N. 2018. Effect of silane coupling on the joint characteristics of friction lap joined Al alloy/CFRP. *Welding International* 32: 328–37. DOI: 10.1080/09507116.2017.1346819

110. Zhao, S., Kimura, F., Kadoya, S., and Kajihara, Y. Experimental analysis on mechanical interlocking of metal-polymer direct joining. *Precision Engineering* 61: 120–5. DOI: 10.1016/j.precisioneng.2019.10.009

111. Saborowski, E., Dittes, A., Steinert, P., Lindner, T., Scharf, I., and Schubert, A., et al. 2019. Effect of metal surface topography on the interlaminar shear and tensile strength of aluminum/polyamide 6 polymer-metal-hybrids. *Materials* 12: 2963.

112. Rodríguez-Vidal, E., Sanz, C., Lambarri, J., and Quintana, I. 2018. Experimental investigation into metal micro-patterning by laser on polymer-metal hybrid joining. *Optics & Laser Technology* 104: 73–82.

113. Kim, W. S., Yun, I. H., Lee, J. J., and Jung, H. T. 2010. Evaluation of mechanical interlock effect on adhesion strength of polymer–metal interfaces using micro-patterned surface topography. *International Journal of Adhesion and Adhesives* 30: 408–17. DOI: 10.1016/j.ijadhadh.2010.05.004

114. Yusof, F., Muhamad, M. R., Moshwan, R., Jamaludin, M. F., and Miyashita, Y. 2016. Effect of surface states on joining mechanisms and mechanical properties of aluminum alloy (A5052) and polyethylene terephthalate (PET) by dissimilar friction spot welding. *Metals* 6: 101. DOI: 10.3390/met6050101

115. Dawei, Z., Qi, Z., Xiaoguang, F., and Shengdun, Z. 2018. Review on joining process of carbon fiber-reinforced polymer and metal: Methods and joining process. *Rare Metal Materials and Engineering* 47: 3686–96. DOI: 10.1016/S1875-5372(19)30018-9

116. Zou, X., Sariyev, B., Chen, K., Jiang, M., Wang, M., and Hua, X., et al. 2021. Enhanced interfacial bonding strength between metal and polymer via synergistic effects of particle anchoring and chemical bonding. *Journal of Manufacturing Processes* 68: 558–68. DOI: 10.1016/j.jmapro.2021.05.058

117. Nasreen, A., Shaker, K., and Nawab, Y. 2021. Effect of surface treatments on metal–composite adhesive bonding for high-performance structures: An overview. *Composite Interfaces* 28: 1221–56. DOI: 10.1080/09276440.2020.1870192

118. Elahi, M. A., Koch, M., Bardon, J., Addiego, F., and Plapper, P. 2021. Failure mechanism analysis based on laser-based sur-face treatments for aluminum-polyamide laser joining. *Journal of Materials Processing Technology* 298: 117318. DOI: 10.1016/j.jmatprotec.2021.117318

119. Steinert, P., Dittes, A., Schimmelpfennig, R., Scharf, I., Lampke, T., and Schubert, A. 2018. Design of high strength polymer metal interfaces by laser microstructured surfaces. *IOP Conference Series Materials Science and Engineering* 373: 12015. DOI: 10.1088/1757-899X/373/1/012015

120. Heckert, A., Singer, C., Zaeh, M. F., Daub, R., and Zeilinger, T. 2016. Gas-tight thermally joined metal-thermoplastic connections by pulsed laser surface pre-treatment. *Physics Procedia* 83: 1083–93. DOI: 10.1016/j.phpro.2016.08.114

121. Lambiase, F., Yanala, P. B., Leone, C., and Paoletti, A. 2023. Influence of laser texturing strategy on thermomechanical joining of AA7075 aluminum alloy and PEEK. *Composite Structure* 315: 116974. DOI: 10.1016/j.compstruct.2023.116974

122. Tan, C., Su, J., Feng, Z., Liu, Y., Chen, B., and Song, X. 2021. Laser joining of CFRTP to titanium alloy via laser surface texturing. *Chinese Journal of Aeronautics* 34: 103–14. DOI: 10.1016/j.cja.2020.08.017

123. Martínez-Viademonte, M. P., Abrahami, S. T., Hack, T., Burchardt, M., and Terryn, H. 2020. A review on anodizing of aerospace aluminum alloys for corrosion protection. *Coatings* 10: 1–30. DOI: 10.3390/coatings10111106

124. Buijnsters, J. G., Zhong, R., Tsyntsaru, N., and Celis, J. P. 2013. Surface wettability of macroporous anodized aluminum oxide. *ACS Applied Materials Interfaces* 5: 3224–33. DOI: 10.1021/am4001425

125. Ramarathnam, G., Libertucci, M., Sadowski, M. M., and North, T. H. 1992. Joining of polymers to metal. *Welding Journal* 71: 483-s.

126. Nagatsuka, K., Xiao, B., Wu, L., Nakata, K., Saeki, S., and Kitamoto, Y., et al. 2018. Resistance spot welding of metal/carbon-fibre-reinforced plastics and applying silane coupling treatment. *Science and Technology of Welding and Joining* 23: 181–6. DOI: 10.1080/13621718.2017.1362159

127. Lee, S. H., Yashiro, H., and Kure-Chu, S. Z. 2021. Effect of silane coupling treatment on the joining and sealing performance between polymer and anodized aluminum alloy. *Korean Journal of Materials Research* 31: 122–31. DOI: 10.3740/MRSK.2021.31.3.122

128. Uetsuji, Y., Yagi, T., and Nakamura, Y. 2020. Interfacial adhesive strength of a silane coupling agent with metals: A first principles study. *Materials Today Communications* 25: 101397. DOI: 10.1016/j.mtcomm.2020.101397

129. Aliasghari, S., Ghorbani, M., Skeldon, P., Karami, H., and Movahedi, M. 2017. Effect of plasma electrolytic oxidation on joining of AA 5052 aluminium alloy to polypropylene using friction stir spot welding. *Surface and Coatings Technology* 313: 274–81. DOI: 10.1016/j.surfcoat.2017.01.084

130. Liu, F. C., Liao, J., Gao, Y., and Nakata, K. 2015. Effect of plasma electrolytic oxidation coating on joining metal to plastic. *Science and Technology of Welding Joining* 20: 291–6. DOI: 10.1179/1362171815Y.0000000012

131. Guezenoc, H., Segui, Y., Thery, S., and Asfardjani, K. 1993. Adhesion characteristics of plasma-treated polypropylene to mild steel. *Journal of Adhesion Science and Technology* 7: 953–65. DOI: 10.1163/156856193X00943

132. Chen, J., Du, K., Chen, X., Li, Y., Huang, J., and Wu, Y., et al. 2019. Influence of surface microstructure on bonding strength of modified polypropylene/aluminum alloy direct adhesion. *Applied Surface Science* 489: 392–402. DOI: 10.1016/j.apsusc.2019.05.270

133. Bahrami, M., Lavayen-Farfan, D., Martínez, M. A., and Abenojar, J. 2022. Experimental and numerical studies of polyamide 11 and 12 surfaces modified by atmospheric pressure plasma treatment. *Surfaces and Interfaces* 32: 102154. DOI: 10.1016/j.surfin.2022.102154

134. Liston, E. M., Martinu, L., and Wertheimer, M. R. 1993. Plasma surface modification of polymers for improved adhesion: A critical review. *Journal of Adhesion Science and Technology* 7: 1091–127. DOI: 10.1163/156856193X00600

135. Shang, S. L., Sun, H., Pan, B., Wang, Y., Krajewski, A. M., and Banu, M., et al. 2021. Forming mechanism of equilibrium and non-equilibrium metallurgical phases in dissimilar aluminum/steel (Al–Fe) joints. *Scientific Reports* 11: 1–15. DOI: 10.1038/s41598-021-03578-0

136. Takenaka, K., Machida, R., Bono, T., Jinda, A., Toko, S., and Uchida, G., et al. 2022. Development of a non-thermal atmospheric pressure plasma-assisted technology for the direct joining of metals with dissimilar materials. *Journal of Manufacturing Processes* 75: 664–9. DOI: 10.1016/j.jmapro.2022.01.041

137. Liang, C. S., Lv, Z. F., Bo, Y., Cui, J. Y., and Xu, S. A. 2015. Effect of modified polypropylene on the interfacial bonding of polymer-aluminum laminated films. *Materials & Design* 81: 141–8. DOI: 10.1016/j.matdes.2015.05.021

138. Tao, W., Su, X., Chen, Y., and Tian, Z. 2019. Joint formation and fracture characteristics of laser welded CFRP/TC4 joints. *Journal of Manufacturing Processes* 45: 1–8. https://doi.org/10.1016/j.jmapro.2019.05.028.

139. Kornacka, E. M., Przybytniak, G., Fuks, L., Walo, M., and Łyczko, K. 2014. Functionalization of polymer surfaces by radiation-induced grafting for separation of heavy metal ions. *Radiation Physics and Chemistry* 94: 115–8. DOI: 10.1016/j.radphyschem.2013.05.047

140. Ku, J. H., Jung, I. H., Rhee, K. Y., and Park, S. J. 2013. Atmospheric pressure plasma treatment of polypropylene to improve the bonding strength of polypropylene/aluminum composites. *Composites Part B: Engineering* 45: 1282–7. DOI: 10.1016/j.compositesb.2012.06.016

141. Chen, M. A., Li, H. Z., and Zhang, X. M. 2007. Improvement of shear strength of aluminium-polypropylene lap joints by grafting maleic anhydride onto polypropylene. *International Journal of Adhesion and Adhesives* 27: 175–87. DOI: 10.1016/j.ijadhadh.2006.01.008

142. Astigarraga, V., Gondra, K., Valea, Á., and Pardo Aurrekoetxea, G. 2019. Improvement of adhesive bonding of polypropylene and maleic anhydride grafted polypropylene blends to aluminium by means of addition of cyclic butylene terephthalate. *The Journal of Adhesion* 95: 286–307. DOI: 10.1080/00218464.2018.1437415

143. Li, C., Zhang, Y., and Zhang, Y. 2003. Melt grafting of maleic anhydride onto low-density polyethylene/polypropylene blends. *Polymer Testing* 22: 191–5. DOI: 10.1016/S0142-9418(02)00079-X

144. Tan, X., Xu, Y., Jia, G., and Qian, J. 2007. Ultrasonically initiated grafting of maleic anhydride onto poly(propylene). *Macromolecular Reaction Engineering* 1: 185–90. DOI: 10.1002/mren.200600012

145. Zhou, J., and Yan, F. 2004. Effect of polyethylene-graft-maleic anhydride as a compatibilizer on the mechanical and tribological behaviors of ultrahigh-molecular-weight polyethylene/copper composites. *Journal of Applied Polymer Science* 93: 948–55 DOI: 10.1002/app.20489

146. Chen, M. A., Zhang, X. M., Huang, R., and Lu, X. 2008. Mechanism of adhesion promotion between aluminium sheet and polypropylene with maleic anhydride-grafted polypropylene by γ-aminopropyltriethoxy silane. *Surface and Interface Analysis* 40: 1209–18. DOI: 10.1002/sia.2871

147. Okada, T., Uchida, S., and Nakata, K. 2014. Direct joining of aluminum alloy and plastic sheets by friction lap processing. *Materials Science Forum* 794–796: 395–400. DOI: 10.4028/www.scientific.net/MSF.794-796.395

148. Zhang, M., Liu, F. C., Liu, Z. Y., Xue, P., Dong, P., and Zhang, H., et al. 2023. Highly stable nanoscale amorphous microstructure at steel-aluminum interface enabled by a new solid-state additive manufacturing method. *Scripta Materialia* 227. DOI: 10.1016/j.scriptamat.2023.115300

149. Khan, A. S., Dong, P., Liu, F. C., and Zhang, Y. 2024. A state-of-the-art review on direct welding of polymer to metal for structural applications: Part 2 - Joint design and property characterization. Submitted to the *Welding Journal*.

ABDUL SAYEED KHAN, **PINGSHA DONG** (*dongp@umich.edu*), **FENGCHAO LIU**, and **YUNING ZHANG** are with the Department of Naval Architecture and Marine Engineering, University of Michigan, Ann Arbor, Mich. **DONG** is also with the Department of Mechanical Engineering, University of Michigan, Ann Arbor, Mich.